

Metric Selection in Douglas-Rachford Splitting and ADMM

Pontus Giselsson* and Stephen Boyd*

Abstract—Recently, several convergence rate results for Douglas-Rachford splitting and the alternating direction method of multipliers (ADMM) have been presented in the literature. In this paper, we show linear convergence of Douglas-Rachford splitting and ADMM under certain assumptions. We also show that the provided bounds on the linear convergence rates generalize and/or improve on similar bounds in the literature. Further, we show how to select the algorithm parameters to optimize the provided linear convergence rate bound. For smooth and strongly convex finite dimensional problems, we show how the linear convergence rate bounds depend on the metric that is used in the algorithm, and we show how to select this metric to optimize the bound. Since most real-world problems are not both smooth and strongly convex, we also propose heuristic metric and parameter selection methods to improve the performance of a much wider class of problems that does not satisfy both these assumptions. These heuristic methods can be applied to problems arising, e.g., in compressed sensing, statistical estimation, model predictive control, and medical imaging. The efficiency of the proposed heuristics is confirmed in a numerical example on a model predictive control problem, where improvements of more than one order of magnitude are observed.

I. INTRODUCTION

Optimization problems of the form

$$\begin{aligned} & \text{minimize} && f(x) + g(y) \\ & \text{subject to} && \mathcal{A}x = y \end{aligned} \quad (1)$$

where $x \in \mathcal{H}$ is the variable, f and g are convex, and \mathcal{A} is a bounded linear operator, arise in numerous applications ranging from compressed sensing [8] and statistical estimation [23] to model predictive control [39] and medical imaging [30]. There exist a variety of algorithms for solving convex problems of the form (1), many of which are treated in the monograph [34]. The methods include primal and dual forward-backward splitting methods [10] and their accelerated variants [4], the Arrow-Hurwicz method [1], Douglas-Rachford splitting [15] and Peaceman-Rachford splitting [36], the alternating direction method of multipliers (ADMM) [22], [18], [7] (which is Douglas-Rachford splitting applied to the dual problem [17], [16]), and linearized ADMM [9].

In this paper, we focus on generalized Douglas-Rachford splitting, which includes Douglas-Rachford splitting and Peaceman-Rachford splitting when applied to the primal and under- and over-relaxed ADMM when applied to the dual. These methods have long been known to converge under very general assumptions, [18], [29], [16]. However, the rate of convergence in the general case has just recently been shown to be $O(1/k)$, [24], [13], [11]. For a restricted class of problems Lions and Mercier showed in [29] that the Douglas-Rachford algorithm enjoys a linear convergence rate. To the

authors's knowledge, this was the sole linear convergence rate results for a long period of time for these methods. Recently, however, many works have shown linear convergence rates for Douglas-Rachford splitting, Peaceman-Rachford splitting and ADMM in different settings [25], [37], [13], [12], [14], [19], [35], [26], [27], [6], [41]. The works in [25], [13], [6], [37] concern local linear convergence under different assumptions. The works in [26], [27], [41] consider distributed formulations, while the works in [12], [14], [19], [35], [29] consider global convergence. The works in [12], [14], [19], [35], [29] are the only ones that provide explicit convergence rate factors that can be optimized by selecting the algorithm parameter. In this paper, we generalize the settings and/or improve on the convergence rate estimates compared to the works [12], [14], [19], [35], [29]. We highlight the improvements compared to [29] in several places in the manuscript, and in Section IV-B we discuss and compare the generalizations and convergence rate improvements compared to [12], [14], [19], [35], [29].

During the submission procedure of this paper, also [38] and [32] that show linear convergence rate bounds of ADMM were published online. In [38] linear convergence is shown under more general assumptions than in the current paper and the other papers mentioned above. The assumptions, however, are more difficult to verify. The rate bounds in [38] are also difficult to compare to since other assumptions are used than in the current paper. In [32] the linear convergence rate bounds are obtained by using the ICQ-framework CITE! The bounds are obtained by solving a small-scale semi-definite program. Also these bounds are slightly more conservative than the ones presented in the current paper. This is shown in Section IV-B. In [32] it is also shown through examples that an over-relaxation with a factor $\alpha \geq 1$ can be used in the linearly convergent case (in the general case, the relaxation factor is limited to $\alpha \in (0, 1)$). No explicit upper bounds on α are given. Such upper bounds are provided in this paper.

When solving problems of the form (1) in finite dimensional Euclidean settings, we can choose a Hilbert space with inner product $\langle \cdot, \cdot \rangle_M$ and induced norm on which to apply the generalized Douglas-Rachford algorithm. The algorithm behaves differently for different choices of M and an appropriate choice can significantly speed up the algorithm, both in theory and in practice. Another contribution of this paper is to show how to select a metric M to optimize the linear convergence rate factor for problems where f is smooth and strongly convex, g is any proper, closed, and convex function, and \mathcal{A} is surjective, i.e., has full row rank. These results are applied to both the primal and dual problems, and therefore apply both to Douglas-Rachford splitting and ADMM (which is Douglas-Rachford splitting on the dual). This generalizes, in several directions, the work in [19] in which corresponding results for ADMM applied to solve quadratic programs with linear

* Electrical Engineering Department, Stanford University. Email: {pontusg,boyd}@stanford.edu

inequality constraints are provided.

Real-world problems rarely have the properties needed to ensure a linear convergence of the generalized Douglas-Rachford algorithm or ADMM. Therefore, we provide heuristic metric and parameter selection methods for cases when some of these assumptions are not met. The heuristics cover most optimization problems that have a quadratic part which is not necessarily strongly convex. Such problems arise, e.g., in model predictive control [39], statistical estimation [23] using, e.g., lasso [42], and compressed sensing [8] which can be used, e.g., in medical imaging [30]. A numerical example on a model predictive control problem is provided that shows the efficiency of the proposed metric selection heuristic. For the considered problem, the execution time is decreased with about one order of magnitude compared to when applying the algorithm on the Euclidean space with the standard inner product and induced norm.

This paper is an extended version of [20]. It extends the results in [20] in that we provide convergence rate results for general Hilbert spaces, as opposed to Euclidean spaces in [20]. Also, we provide a much more detailed analysis that sheds light on why our linear convergence rates are better than most other rates available in the literature.

A. Notation

We denote by \mathbf{R} the set of real numbers, \mathbf{R}^n the set of real column-vectors of length n , and $\mathbf{R}^{m \times n}$ the set of real matrices with m rows and n columns. Further $\overline{\mathbf{R}} := \mathbf{R} \cup \{\infty\}$ denotes the extended real line. We use notation \mathbf{S}^n for symmetric $n \times n$ -matrices and \mathbf{S}_{++}^n [\mathbf{S}_+^n] for positive [semi] definite matrices. Throughout this paper \mathcal{H} denotes a real Hilbert space. Its inner product is denoted by $\langle \cdot, \cdot \rangle$, the induced norm by $\|\cdot\|$, and the identity operator by Id . We specifically consider finite-dimensional Hilbert-spaces \mathbb{H}_H with inner product $\langle x, y \rangle = x^T H y$ and induced norm $\|x\| = \sqrt{x^T H x}$. Sometimes the notation $\langle \cdot, \cdot \rangle_H$ and $\|\cdot\|_H$ is used, while sometimes we use the generic notation where the space they refer to should be clear from the context. We also sometimes denote the Euclidean inner-product by $\langle \cdot, \cdot \rangle_2$ and the induced norm by $\|\cdot\|_2$ for clarity. Finally, the class of closed, proper, and convex functions $f : \mathcal{H} \rightarrow \overline{\mathbf{R}}$ is denoted by $\Gamma_0(\mathcal{H})$.

II. OPERATOR THEORY

In this section, we introduce some definitions and preliminary results in operator theory that will be used later to prove convergence rate results for the Douglas-Rachford algorithm. The definitions stated here are standard and can be found, e.g. in [3], [40]. We supplement many definitions with graphical representations with the intention to clarify concepts and provide intuition to the obtained results.

A. Operator definitions and properties

Throughout this section, we suppose that \mathcal{X} and \mathcal{Y} are nonempty sets.

Definition 1 (Power set): The power set of \mathcal{X} is the set of all subsets of \mathcal{X} and is denoted by $2^{\mathcal{X}}$.

Definition 2 (Operators): An operator (or mapping) $A : \mathcal{X} \rightarrow \mathcal{Y}$ maps each point in \mathcal{X} to a point in \mathcal{Y} .

We denote by Ax and $A(x)$ the point in \mathcal{Y} that results from applying the operator A on x .

Definition 3 (Set-valued operators): A set-valued operator $A : \mathcal{X} \rightarrow 2^{\mathcal{Y}}$ maps each element in \mathcal{X} to a set in \mathcal{Y} .

For set-valued operators, we denote by $A(x)$ and Ax the set in \mathcal{Y} that results from applying the operator A on x . This set might be the empty-set since $\emptyset \in 2^{\mathcal{Y}}$. If Ax is a singleton or the empty-set for all $x \in \mathcal{X}$, the operator A is at most *single-valued*. In such cases, by letting $\mathcal{D} \subseteq \mathcal{X}$ be a subset of \mathcal{X} , the set-valued operator A can be associated with an operator $B : \mathcal{D} \rightarrow \mathcal{Y}$ that satisfies $Bx = Ax$ for all $x \in \mathcal{D}$ and where $Ax = \emptyset$ for the remaining $x \in \mathcal{X} \setminus \mathcal{D}$. With slight abuse of notation, we treat the at most single-valued operator A and its associated operator B to be the same. That is, we let Ax and $A(x)$ denote the point in \mathcal{Y} that results from applying A on $x \in \mathcal{D}$ as well as the singleton set in $2^{\mathcal{Y}}$ that contains the point Bx .

Definition 4 (Graph of an operator): The graph of a set-valued operator $A : \mathcal{X} \rightarrow 2^{\mathcal{Y}}$ is defined as

$$\text{gph}(A) := \{(x, u) \in \mathcal{X} \times \mathcal{Y} \mid u \in A(x)\}.$$

Any set-valued operator is (uniquely) characterized by its graph.

Definition 5 (Inverse operator): The inverse operator of $A : \mathcal{X} \rightarrow 2^{\mathcal{Y}}$ is denoted by $A^{-1} : \mathcal{Y} \rightarrow 2^{\mathcal{X}}$ and is described through its graph

$$\text{gph}(A^{-1}) := \{(u, x) \in \mathcal{Y} \times \mathcal{X} \mid (x, u) \in \text{gph}(A)\}.$$

This definition implies that for any pair of points (x, u) , we have that $u \in A(x)$ is equivalent to $x \in A^{-1}(u)$.

Definition 6 (Fixed-points): The set of fixed-points for a mapping $A : \mathcal{X} \rightarrow \mathcal{X}$ is defined as

$$\text{fix}A = \{x \in \mathcal{X} \mid x = Ax\}.$$

Definition 7 (Strong convergence): A sequence of points $\{x_k\}_{k=0}^{\infty}$ converges *strongly* to a point x if $\|x^k - x\| \rightarrow 0$ as $k \rightarrow \infty$.

In this paper, the term convergence always refers to strong convergence.

Next, we state some properties for operators. Graphical representations of these properties are provided in Figure 1.

Definition 8 (Monotonicity): An operator $A : \mathcal{H} \rightarrow 2^{\mathcal{H}}$ is *monotone* if

$$\langle u - v, x - y \rangle \geq 0$$

for all $(x, u) \in \text{gph}(A)$ and $(y, v) \in \text{gph}(A)$.

Definition 9 (Strong monotonicity): An operator $A : \mathcal{H} \rightarrow 2^{\mathcal{H}}$ is *σ -strongly monotone* if

$$\langle u - v, x - y \rangle \geq \sigma \|x - y\|^2$$

for all $(x, u) \in \text{gph}(A)$ and $(y, v) \in \text{gph}(A)$.

Strong monotonicity is depicted in Figure 1(a). For the graphical representation, we assume that the operator $A : \mathbf{R}^2 \rightarrow \mathbf{R}^2$ is at most single-valued and has a fixed-point.

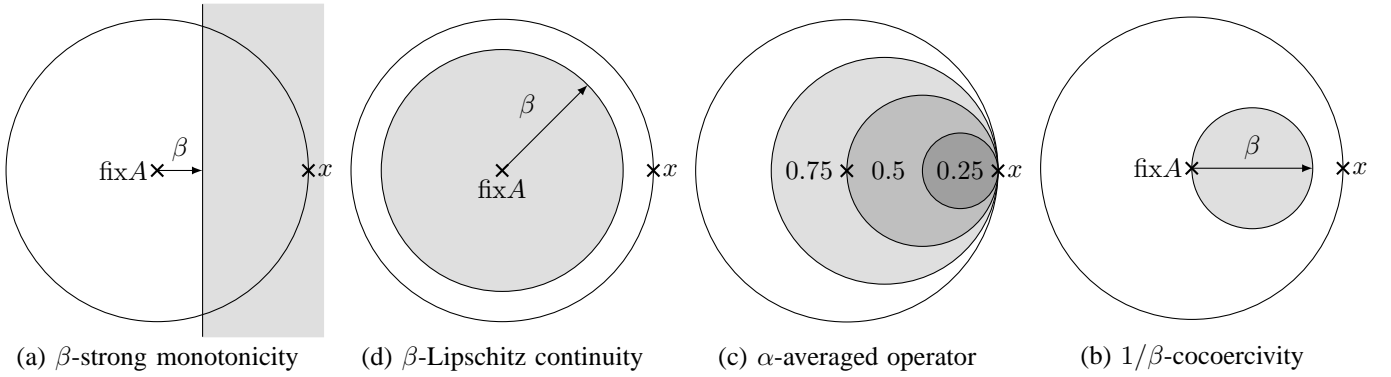


Fig. 1. Graphical representations for (a) strong monotonicity, (b) Lipschitz continuity, (c) α -averaged nonexpansiveness with $\alpha = 0.25, 0.5, 0.75$, and (d) cocoercivity. We suppose that the operator $A : \mathbf{R}^2 \rightarrow \mathbf{R}^2$ has a fixed-point and that $\text{fix}A$ denotes any of these fixed-points in the figures. This fixed-point is in the middle of each figure (even though not explicitly marked in (c)). We also assume that x is on the unit-circle. The point/set Ax is located somewhere inside the gray shaded area in each figure.

Any of these fixed-points is the mid-point in Figure 1(a) and is denoted by $\text{fix}A$. The circle in Figure 1(a) is the unit circle, and the point x is the point on which the operator A operates. The gray area depicts the region within which the set $A(x)$ is contained. The graphical representation of monotonicity is obtained by letting the vertical line defining the border of the gray region intersect with the point $\text{fix}A$ (i.e., when $\beta = 0$).

Definition 10 (Maximal monotonicity): A monotone operator $A : \mathcal{H} \rightarrow 2^{\mathcal{H}}$ is *maximal monotone* if $\text{gph}(A)$ is not a proper subset of the graph of any other monotone operator $B : \mathcal{H} \rightarrow 2^{\mathcal{H}}$.

A way to guarantee maximal monotonicity is to ensure that no pair of points can be added to $\text{gph}(A)$ without violating the monotonicity definition in Definition 8.

In the following definitions, we suppose that $\mathcal{D} \subseteq \mathcal{H}$ is a nonempty subset of \mathcal{H} .

Definition 11 (Lipschitz continuity): A mapping $A : \mathcal{D} \rightarrow \mathcal{H}$ is β -Lipschitz continuous if

$$\|A(x) - A(y)\| \leq \beta \|x - y\|$$

holds for all $x, y \in \mathcal{D}$. If $\beta = 1$ then A is *nonexpansive* and if $\beta \in (0, 1)$ then A is β -contractive.

Lipschitz continuity is depicted in Figure 1(b). From the figure, we see that for $\beta < 1$, i.e., for contractions, the distance to a fixed-point from Ax is strictly smaller than the distance to the fixed-point from x . It can be shown that when iterating a contraction mapping, we get a linear convergence towards the fixed-point. For non-expansive mappings, i.e., with $\beta = 1$, the distance is non-increasing, but there are no decrease guarantees. Thus, when iterating a nonexpansive operator, we are not guaranteed to reach a fixed-point. To find a fixed-point of a nonexpansive operator, averaged operators can be used.

Definition 12 (Averaged mappings): A mapping $A : \mathcal{D} \rightarrow \mathcal{H}$ is α -averaged if there exist a nonexpansive mapping $B : \mathcal{D} \rightarrow \mathcal{H}$ and $\alpha \in (0, 1)$ such that $A = (1 - \alpha)\text{Id} + \alpha B$.

An averaged mapping (or operator) is depicted in Figure 1(c) for different α . In an averaged operator, the point Ax ends up somewhere on the straight line between the points x and Bx (which can be at the unit circle) where the fraction of the distance is decided by the scalar α . Thus, the point

$Ax = ((1 - \alpha)\text{Id} + \alpha B)x$ is strictly inside the unit circle, i.e., the distance to the fixed-point from Ax is strictly smaller than the distance from x . It can be shown [11] that when iterating an averaged nonexpansive operator according to $x^{k+1} = A(x^k)$, then $\{Bx^k - x^k\}$ converges towards 0 with a $O(1/k)$ -rate.

Definition 13 (Cocoercivity): A mapping $A : \mathcal{D} \rightarrow \mathcal{H}$ is β -cocoercive if

$$\langle A(x) - A(y), x - y \rangle \geq \beta \|A(x) - A(y)\|^2$$

holds for all $x, y \in \mathcal{D}$.

Cocoercivity is depicted in Figure 1(d). A 1-cocoercive mapping is equivalent to a $\frac{1}{2}$ -averaged mapping. This can be seen in Figure 1 for the two-dimensional case. Mappings that are 1-cocoercive (or equivalently $\frac{1}{2}$ -averaged) are called *firmly nonexpansive*.

B. Function definitions and properties

In this section, we introduce some functions and list different function properties. We start with convexity.

Definition 14 (Convexity): A function $f : \mathcal{H} \rightarrow \overline{\mathbf{R}}$ is *convex* if

$$f(x) \geq f(y) + \langle u, x - y \rangle$$

hold for all $x, y \in \mathcal{H}$ and all $u \in \partial f(y)$.

Convex functions that are also closed and proper (i.e., not ∞ everywhere) play an important role in optimization. One reason is that the subdifferential ∂f of a proper, closed, and convex function $f : \mathcal{H} \rightarrow \overline{\mathbf{R}}$ is a maximal monotone operator [3, Theorem 21.2]. In this paper, we denote the class of proper, closed, and convex functions $f : \mathcal{H} \rightarrow \overline{\mathbf{R}}$ by $\Gamma_0(\mathcal{H})$.

Definition 15 (Strong convexity): A function $f \in \Gamma_0(\mathcal{H})$ is β -strongly convex if

$$f(x) \geq f(y) + \langle u, x - y \rangle + \frac{\beta}{2} \|x - y\|^2$$

holds for all $x, y \in \mathcal{H}$ and all $u \in \partial f(y)$.

A strongly convex function has a minimum curvature that is decided by β . Functions with a maximal curvature are called smooth. Next, we present smoothness definitions for general (non-convex) functions and for convex functions.

Definition 16 (Smoothness for general functions): A general (nonconvex), closed function $f : \mathcal{H} \rightarrow \mathbf{R}$ is β -smooth if it is differentiable and

$$|f(x) - f(y) - \langle \nabla f(y), x - y \rangle| \leq \frac{\beta}{2} \|x - y\|^2 \quad (2)$$

holds for all $x, y \in \mathcal{H}$.

For convex functions, this definition can be stated as follows by noting that the expression inside the absolute value is always nonnegative, see Definition 14.

Definition 17 (Smoothness for convex functions): A function $f \in \Gamma_0(\mathcal{H})$ is β -smooth if it is differentiable and

$$f(x) \leq f(y) + \langle \nabla f(y), x - y \rangle + \frac{\beta}{2} \|x - y\|^2 \quad (3)$$

holds for all $x, y \in \mathcal{H}$.

We conclude this section by defining the conjugate function.

Definition 18 (Conjugate functions): The conjugate function to $f \in \Gamma_0(\mathcal{H})$ is defined as

$$f^*(y) \triangleq \sup_x \{ \langle y, x \rangle - f(x) \}.$$

The conjugate function will play an important role when analyzing properties of the proximal operator that will be introduced in Section III. Note also that the definition of the conjugate function is dependent on which space the function f is defined since the conjugate depends on the inner product.

C. Duality results

In this section, we will state some duality results that are instrumental in proving the linear convergence rate results for Douglas-Rachford splitting. We start with some properties for the conjugate function that are proven in [3, Corollary 13.33, Corollary 16.24]

Proposition 1: Assume that $f \in \Gamma_0(\mathcal{H})$. Then the following holds:

- (i) The conjugate function $f^* \in \Gamma_0(\mathcal{H})$.
- (ii) The *bi-conjugate* $(f^*)^*$ satisfies $(f^*)^* = f$.
- (iii) The subdifferential of the conjugate function satisfies $\partial f^* = (\partial f)^{-1}$.

The first property implies that ∂f^* is a maximal monotone operator if $f \in \Gamma_0(\mathcal{H})$. The third property says that this maximal monotone operator is the inverse operator of ∂f .

Next, we state some duality results for A and its inverse A^{-1} .

Proposition 2: Consider the following list of properties for $A : \mathcal{H} \rightarrow 2^{\mathcal{H}}$ and its inverse $A^{-1} : \mathcal{D} \rightarrow \mathcal{H}$, where $\mathcal{D} \subseteq \mathcal{H}$ is a subset of \mathcal{H} :

- (i) A is β -strongly monotone.
- (ii) A^{-1} is β -cocoercive.
- (iii) A^{-1} is $\frac{1}{\beta}$ -Lipschitz continuous.

We have (i) \Leftrightarrow (ii) and (ii) \Rightarrow (iii).

Proof. The equivalence (i) \Leftrightarrow (ii) follows directly from the definitions of strong monotonicity (Definition 9) and cocoercivity (Definition 13) and the definition of the inverse operator (Definition 5). The implication (ii) \Rightarrow (iii) follows directly from the Cauchy-Schwarz inequality and the definitions of cocoercivity (Definition 13) and Lipschitz continuity (Definition 11). \square

Note that A^{-1} is defined as an operator $A^{-1} : \mathcal{D} \rightarrow \mathcal{H}$ instead of $A^{-1} : \mathcal{H} \rightarrow 2^{\mathcal{H}}$. This is done for convenience since cocoercivity and Lipschitz continuity implies that the operator is at most single-valued. Also note that the implication (ii) \Rightarrow (iii) can be seen to hold in the two-dimensional Euclidean case in Figure 1, since the gray $\frac{1}{\beta}$ -cocoercivity circle in Figure 1(d) fits inside the gray β -Lipschitz continuity circle in Figure 1(b).

In the following proposition, we show an implication of Lipschitz continuity.

Proposition 3: Suppose that $A : \mathcal{D} \rightarrow \mathcal{H}$ is β -Lipschitz continuous. Then $A^{-1} : \mathcal{H} \rightarrow 2^{\mathcal{H}}$ satisfies

$$\|u - v\| \geq \frac{1}{\beta} \|x - y\|$$

for all $(x, u) \in \text{gph}A^{-1}$ and $(y, v) \in \text{gph}A^{-1}$.

Proof. This result follows directly by the definition of the inverse operator (Definition 5) and the definition of Lipschitz continuity (Definition 11). \square

This property, which we call *inverse Lipschitz continuity*, can be graphically represented using the representation of Lipschitz continuity in Figure 1(b). In the figure, the set $A^{-1}(x)$ ends up *outside* the gray Lipschitz circle, where the gray Lipschitz circle has radius $\frac{1}{\beta}$.

The properties in Propositions 2 and 3 can be sharpened when A is the subdifferential of a proper, closed, and convex function.

Proposition 4: Suppose that $f \in \Gamma_0(\mathcal{H})$. Then the following are equivalent:

- (i) f is β -strongly convex.
- (ii) ∂f is β -strongly monotone.
- (iii) ∇f^* is β -cocoercive.
- (iv) ∇f^* is $\frac{1}{\beta}$ -Lipschitz continuous.
- (v) f^* is $\frac{1}{\beta}$ -smooth.

A proof is provided in [3, Theorem 18.15].

Corollary 1: The converse statement (i.e., with f and f^* interchanged) also holds for $f \in \Gamma_0(\mathcal{H})$ since $f = (f^*)^*$, see Proposition 1.

This result shows that the subdifferential operator is special, since Lipschitz continuity implies cocoercivity, i.e. (iv) \Rightarrow (iii) in Proposition 4. This result, which is due to Baillon and Haddad in [2], is not true for general A , i.e. (iii) $\not\Rightarrow$ (ii) in Proposition 2. The implication (iv) \Rightarrow (iii) in Proposition 4 will be the key when we in this paper improve the convergence rate estimates when minimizing the sum of two convex functions using Douglas-Rachford splitting, compared to when finding a zero of the sum of two general maximal monotone operators, a convergence rate of which was provided in [29].

The final result of this section is that the equivalence (iv) \Leftrightarrow (v) in Proposition 4 holds also for general nonconvex functions.

Proposition 5: Suppose that $f : \mathcal{H} \rightarrow \mathbf{R}$. Then the following are equivalent:

- (i) ∇f is β -Lipschitz continuous.
- (ii) f is β -smooth.

A proof to this is provided in Appendix A.

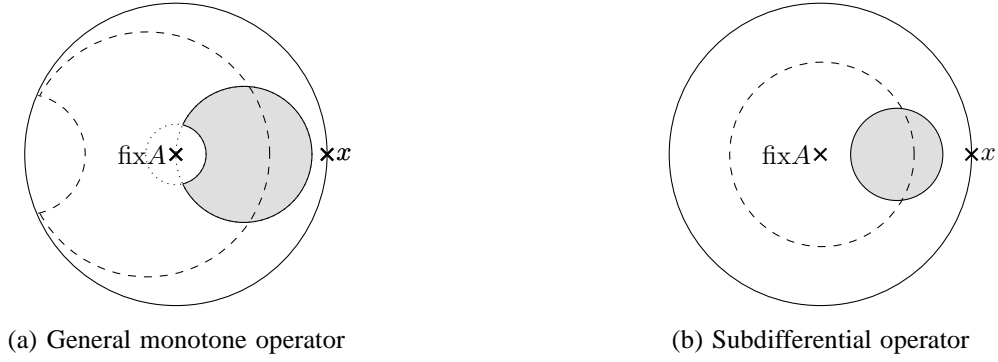


Fig. 2. Graphical representations for the resolvent and reflected resolvent for a $1/9$ -strongly monotone and 4 -Lipschitz continuous general maximal monotone operator $\gamma A : \mathbf{R}^2 \rightarrow 2^{\mathbf{R}^2}$ in (a) and subdifferential operator $\gamma \partial f : \mathbf{R}^2 \rightarrow 2^{\mathbf{R}^2}$ in (b), where $\gamma = 1$ in both cases. The gray regions show where the resolvent/proximal operator can end up, and the dashed regions show where the reflected resolvent/reflected proximal operator can end up. The contraction factors for the reflected resolvent and the reflected proximal operator are 0.991 and 0.8 respectively.

III. IMPORTANT OPERATORS

In this section, we will introduce some operators that are used in the Douglas-Rachford algorithm. We will also state properties of these operators that will allow us to show linear convergence of the algorithm.

Definition 19 (Resolvents): Let \mathcal{D} be a subset of \mathcal{H} . Then the *resolvent* $J_A : \mathcal{D} \rightarrow \mathcal{H}$ of a monotone operator $A : \mathcal{H} \rightarrow 2^{\mathcal{H}}$ is defined as

$$J_A := (I + A)^{-1}.$$

Since $(I + A)$ is 1 -strongly monotone, Proposition 2 implies that $J_A = (I + A)^{-1}$ is 1 -cocoercive, i.e., firmly nonexpansive, and, as such, at most single-valued. Therefore the resolvent is defined on $J_A : \mathcal{D} \rightarrow \mathcal{H}$ instead of $J_A : \mathcal{H} \rightarrow 2^{\mathcal{H}}$. If in addition A is maximally monotone, the resolvent has full domain, i.e. $\mathcal{D} = \mathcal{H}$ and $J_A : \mathcal{H} \rightarrow \mathcal{H}$, see [3, Theorem 21.1]. This property is crucial when using the resolvent in an algorithm, since the resolvent can operate on any point and give a unique point back. Next, we state properties for the resolvent under strong monotonicity assumptions and Lipschitz continuity assumptions.

Proposition 6: Suppose that $A : \mathcal{H} \rightarrow 2^{\mathcal{H}}$ is a σ -strongly monotone and maximal operator. Then the resolvent $J_A : \mathcal{H} \rightarrow \mathcal{H}$ is $(1 + \sigma)$ -cocoercive, and $\frac{1}{1 + \sigma}$ -Lipschitz continuous.

Proof. This follows directly from Proposition 2 by noting that $I + A$ is $(1 + \sigma)$ -strongly monotone. \square

Proposition 7: Suppose that $A : \mathcal{H} \rightarrow \mathcal{H}$ is a β -Lipschitz continuous and maximal operator. Then the resolvent $J_A : \mathcal{H} \rightarrow \mathcal{H}$ satisfies

$$\|J_A(x) - J_A(y)\| \geq \frac{1}{1 + \beta} \|x - y\|$$

for all $x, y \in \mathcal{H}$.

Proof. This follows directly from Proposition 3 and by noting that $A + I$ is $(1 + \beta)$ -Lipschitz continuous. \square

The cocoercivity property is graphically represented in Figure 1(d) and the inverse Lipschitz property is graphically represented as the region *outside* the Lipschitz circle in Figure 1(b). If the maximal monotone operator A is both σ -strongly monotone, and β -Lipschitz continuous, Figure 2(a)

shows in which area (the gray area) the resolvent can end up. The figure is obtained by intersecting the $(1 - \sigma)$ -cocoercivity circle and the $\frac{1}{1 + \beta}$ -inverse Lipschitz region.

In the special case where the operator is a positive scalar times the subdifferential of a proper, closed, and convex function, the resolvent is called the proximal operator.

Definition 20 (Proximal operators): The *proximal operator* of a function $f \in \Gamma_0(\mathcal{H})$ is given by

$$\text{prox}_{\gamma f}(y) := \underset{x}{\operatorname{argmin}} \left\{ f(x) + \frac{1}{2\gamma} \|x - y\|^2 \right\}.$$

To see that the prox operator is indeed the resolvent of $\gamma \partial f$, we let $x^* = \text{prox}_{\gamma f}(y)$ and state the optimality conditions:

$$\begin{aligned} 0 &\in \partial f(x^*) + \gamma^{-1}(x^* - y) \\ \Leftrightarrow y &\in (\text{Id} + \gamma \partial f)x^* \\ \Leftrightarrow x^* &\in (\text{Id} + \gamma \partial f)^{-1}y. \end{aligned}$$

Since the subdifferential is a maximal monotone operator, [3, Theorem 21.1] shows that the proximal operator has full domain, i.e., $\text{prox}_{\gamma f} : \mathcal{H} \rightarrow \mathcal{H}$.

We will also use another description of the proximal operator, namely that it is the gradient of the conjugate of the function $f_\gamma : \mathcal{H} \rightarrow \overline{\mathbf{R}}$ defined as

$$f_\gamma := \gamma f + \frac{1}{2} \|\cdot\|^2 \quad (4)$$

where $\gamma > 0$. The function f_γ is the scaled original function with quadratic norm regularization. That the prox operator is indeed the gradient of the conjugate of f_γ is shown in the following proposition.

Proposition 8: Assume that $f \in \Gamma_0(\mathcal{H})$, then $\text{prox}_{\gamma f}(y) = \nabla f_\gamma^*(y)$, where f_γ is defined in (4).

Proof. We have $\text{prox}_{\gamma f}(y) = (\text{Id} + \gamma \partial f)^{-1}y = (\partial f_\gamma)^{-1}y = \nabla f_\gamma^*(y)$, where the last step follows from Proposition 1. Since f_γ is 1 -strongly convex, Proposition 4 implies that f_γ^* is smooth, hence differentiable. \square

This relation between the proximal operator and the gradient of the conjugate of a strongly convex function can be used to derive properties of the proximal operator. This is done next.

Proposition 9: Assume that $f \in \Gamma_0(\mathcal{H})$ is σ -strongly convex. Then $\text{prox}_{\gamma f} : \mathcal{H} \rightarrow \mathcal{H}$ is $(1 + \gamma\sigma)$ -cocoercive and $\frac{1}{1+\gamma\sigma}$ -contractive.

Proof. By noting that $\gamma\partial f$ is $\gamma\sigma$ -strongly monotone, this follows directly from Proposition 8 and Proposition 4. \square

Proposition 10: Assume that $f \in \Gamma_0(\mathcal{H})$ is β -smooth. Then $\text{prox}_{\gamma f} : \mathcal{H} \rightarrow \mathcal{H}$ is $\frac{1}{1+\gamma\beta}$ -strongly monotone.

Proof. Since f is β -smooth, f_γ is $(1 + \gamma\beta)$ -smooth. Apply Propositions 8 and 4 to get the result. \square

Next, we state a result that shows properties of the prox operator if f is both strongly convex and smooth.

Proposition 11: Assume that $f \in \Gamma_0(\mathcal{H})$ is σ -strongly convex and β -smooth. Then $\text{prox}_{\gamma f} - \frac{1}{1+\gamma\beta}I$ is $\frac{1}{\frac{1}{1+\gamma\sigma} - \frac{1}{1+\gamma\beta}}$ -cocoercive.

Proof. Since f is σ -strongly convex and β -smooth, Propositions 8, 9, 10, and 4 imply that f_γ^* is $\frac{1}{1+\gamma\sigma}$ -smooth and $\frac{1}{1+\gamma\beta}$ -strongly convex. Multiply the equality

$$\frac{1}{2}\|x\|^2 = \frac{1}{2}\|y\|^2 + \langle y, x - y \rangle + \frac{1}{2}\|x - y\|^2$$

by $\frac{1}{1-\gamma\beta}$, add to the smoothness definition of f_γ^* in (3) using smoothness parameter $\frac{1}{1+\gamma\sigma}$, and define $\phi = f_\gamma^* - \frac{1}{2(1-\gamma\beta)}\|\cdot\|^2$ to get

$$\phi(x) \leq \phi(y) + \langle \phi(y), x - y \rangle + \frac{1}{2}\left(\frac{1}{1-\gamma\sigma} - \frac{1}{1-\gamma\beta}\right)\|x - y\|^2.$$

That is, ϕ is $(\frac{1}{1-\gamma\sigma} - \frac{1}{1-\gamma\beta})$ -smooth and Proposition 4 gives the result. \square

The region of points for which the prox operator can end up if f is β -smooth and σ -strongly convex is depicted in Figure 2(b). This region is strictly smaller than the corresponding region for general maximal monotone operators in Figure 2(a). This decrease in region size is due to the sharpening in Proposition 10 compared to Proposition 7, and enables for improved convergence rate estimates in the setting of minimizing the sum of two proper, closed, and convex function, as we will see later.

Next, we introduce the reflected resolvent.

Definition 21 (Reflected resolvent): The reflected resolvent of an operator $A : \mathcal{H} \rightarrow 2^{\mathcal{H}}$ is defined as

$$R_A := 2J_A - \text{Id}.$$

If A is maximally monotone, then R_A has full domain, i.e., $R_A : \mathcal{H} \rightarrow \mathcal{H}$, since the resolvent J_A has full domain in that case.

In the general case, the reflected resolvent is nonexpansive, see [3, Proposition 4.2]. Intuition of this can be gained by the graphical representations in Figures 1(c), and 1(d). The reason is that the resolvent is 1-cocoercive, or equivalently $\frac{1}{2}$ -averaged. By multiplying the corresponding circles by two (radially outward from the fixed-point) and shifting by $-I$ gives a gray circle that covers the unit circle. In the case of A being Lipschitz continuous and strongly monotone, we get the following tighter result.

Proposition 12: Suppose that $A : \mathcal{H} \rightarrow \mathcal{H}$ is σ -strongly monotone and β -Lipschitz continuous. Then R_A is $\sqrt{1 - \frac{4\sigma}{(1+\beta)^2}}$ -contractive.

Proof. We have

$$\begin{aligned} \|R_A x - R_A y\|^2 &= \|2J_A x - 2J_A y - (x - y)\|^2 \\ &= 4\|J_A x - J_A y\|^2 - 4\langle J_A x - J_A y, x - y \rangle + \|x - y\|^2 \\ &\leq 4\|J_A x - J_A y\|^2 - 4(1 + \sigma)\|J_A x - J_A y\|^2 + \|x - y\|^2 \\ &= -4\sigma\|J_A x - J_A y\|^2 + \|x - y\|^2 \\ &\leq \left(1 - \frac{4\sigma}{(1 + \beta)^2}\right)\|x - y\|^2 \end{aligned}$$

where the first inequality comes from Proposition 6 and the second from Proposition 7. \square

This is essentially the result on which the linear convergence rate in [29] is based. The region within which the reflected resolvent can end up when A is both strongly monotone and Lipschitz continuous is shown in dashed in Figure 2(a). This region is obtained by multiplying the gray resolvent region in the figure by two and shifting by $-I$. The contraction factor is given by the distance between the intersection of the two dashed circles and the fixed-point.

Finally, we introduce the reflected proximal operator as a special case of the reflected resolvent.

Definition 22: The *reflected proximal operator* to $f \in \Gamma_0(\mathcal{H})$ is defined as

$$R_{\gamma f} := 2\text{prox}_{\gamma f} - \text{Id}.$$

With slight abuse of notation, we use $R_{\gamma f} = R_{\gamma\partial f}$, i.e., both refer to the reflected proximal operator. In the general case, the reflected proximal operator and the reflected resolvent have the same properties, i.e., they are nonexpansive. However, if ∂f is both strongly monotone and Lipschitz continuous, the contraction factor of the reflected proximal operator is significantly smaller. This is shown in the following proposition which is proven in Appendix B.

Proposition 13: Suppose that f is σ -strongly convex and β -smooth. Then $R_{\gamma f}$ is $\max(\frac{\gamma\beta-1}{\gamma\beta+1}, \frac{1-\gamma\sigma}{\gamma\sigma+1})$ -Lipschitz continuous.

The dashed region in Figure 2(b) shows where the reflected resolvent can end up if f is strongly convex and Lipschitz continuous. The contraction factor is given by the distance between the part of the dashed circle that is farthest away from the fixed-point and the fixed-point itself. We see that for the same values of β and σ , the contraction factor in the subdifferential case in Figure 2(b) is significantly smaller than in the general monotone operator case in Figure 2(a). This is the reason why we can significantly improve the convergence rate estimates compared to the results in [29].

IV. GENERALIZED DOUGLAS-RACHFORD SPLITTING

The generalized Douglas-Rachford algorithm can be applied to solve inclusion problems of the form

$$0 \in A(x) + B(x) \quad (5)$$

where $A : \mathcal{H} \rightarrow 2^{\mathcal{H}}$ and $B : \mathcal{H} \rightarrow 2^{\mathcal{H}}$ are maximal monotone operators. The solution to (5) is characterized by the following optimality conditions, [3, Proposition 25.1]

$$z = R_{\gamma A} R_{\gamma B} z, \quad x = J_{\gamma B} z$$

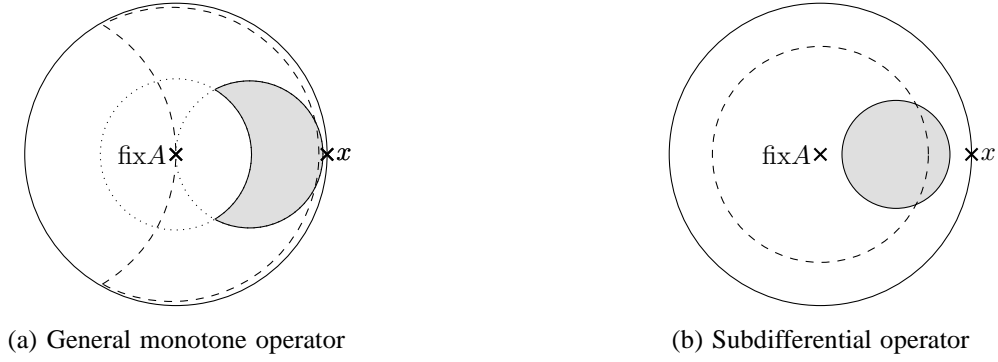


Fig. 3. Graphical representations for the resolvent and reflected resolvent for a $1/9$ -strongly monotone and 4 -Lipschitz continuous general maximal monotone operator $\gamma A : \mathbf{R}^2 \rightarrow 2\mathbf{R}^2$ in (a) and subdifferential operator $\gamma \partial f : \mathbf{R}^2 \rightarrow 2\mathbf{R}^2$ in (b), with γ that optimizes the respective contraction factors, i.e., $\gamma = 1/\beta = 1/4$ in (a) and $\gamma = 1/\sqrt{\sigma\beta} = 1/\sqrt{4/9}$ in (b). The gray regions show where the resolvent/proximal operator can end up, and the dashed regions show where the reflected resolvent/reflected proximal operator can end up. The contraction factors for the reflected resolvent and the reflected proximal operator are 0.986 and 0.7 respectively.

where $\gamma > 0$. In other words, the solution to (5) is found by applying the resolvent of A on z , where z is a fixed-point to $R_{\gamma A}R_{\gamma B}$. One approach to find a fixed-point to $R_{\gamma A}R_{\gamma B}$ is to iterate the composition:

$$z^{k+1} = R_{\gamma A}R_{\gamma B}z^k.$$

This algorithm is known as Peaceman-Rachford splitting. However, since $R_{\gamma A}$ and $R_{\gamma B}$ are nonexpansive, so is their composition, and convergence of this algorithm cannot be guaranteed in the general case. The generalized Douglas-Rachford splitting algorithm is obtained by introducing averaging to the nonexpansive Peaceman-Rachford operator $R_{\gamma A}R_{\gamma B}$. That is, it is given by the iteration

$$z^{k+1} = ((1 - \alpha)\text{Id} + \alpha R_{\gamma A}R_{\gamma B})z^k \quad (6)$$

where $\alpha \in (0, 1)$, or more explicitly

$$x^k = J_{\gamma A}(z^k) \quad (7)$$

$$y^k = J_{\gamma B}(2x^k - z^k) \quad (8)$$

$$z^{k+1} = z^k + 2\alpha(y^k - x^k) \quad (9)$$

Since (6) is an averaged iteration of a nonexpansive mapping (see Figure 1(c) for a graphical representation of averaged operators), the sequence $\{z^k - R_{\gamma A}R_{\gamma B}z^k\}$ converges to 0, if a fixed-point to $R_{\gamma A}R_{\gamma B}$ exists, see [3, Theorem 5.14]. The algorithm known as Douglas-Rachford splitting is obtained by letting $\alpha = \frac{1}{2}$ in (6).

A. Linear convergence

For some problem classes, the convergence rate of generalized Douglas-Rachford splitting is linear. This is shown in the following proposition, which is a slight improvement and generalization of the corresponding result in [29, Proposition 4].

Proposition 14: Suppose that $A : \mathcal{H} \rightarrow \mathcal{H}$ and $B : \mathcal{H} \rightarrow 2\mathcal{H}$ are maximal monotone operators and that A is σ -strongly monotone and β -Lipschitz continuous. Then the generalized Douglas Rachford algorithm (6) converges linearly to a point

$\bar{z} \in \text{fix}(R_{\gamma A}R_{\gamma B})$ with rate $|1 - \alpha| + \alpha\sqrt{1 - \frac{4\gamma\sigma}{(1+\gamma\beta)^2}}$, i.e.

$$\|z^{k+1} - \bar{z}\| \leq \left(|1 - \alpha| + \alpha\sqrt{1 - \frac{4\gamma\sigma}{(1+\gamma\beta)^2}}\right)^k \|z^0 - \bar{z}\|. \quad (10)$$

For a proof, see Appendix C.

Remark 1: As we will see, this result implies that $\alpha > 1$ can be chosen. A similar finding is reported in [32], but no explicit expression for α is provided. To get a linear convergence, the rate factor should be less than 1, i.e.

$$\begin{aligned} & |1 - \alpha| + \alpha\sqrt{1 - \frac{4\gamma\sigma}{(1+\gamma\beta)^2}} < 1 \\ \Leftrightarrow & \frac{2}{1 + \sqrt{1 - \frac{4\gamma\sigma}{(1+\gamma\beta)^2}}} > \alpha. \end{aligned}$$

This is an explicit upper bound for α which is > 1 whenever $\sigma > 0$.

The rate bound in Proposition 14 depends explicitly on the parameters γ and α . Thus, the parameters γ and α can be chosen to optimize the bound. This is done in the following proposition.

Proposition 15: Suppose that $A : \mathcal{H} \rightarrow \mathcal{H}$ and $B : \mathcal{H} \rightarrow 2\mathcal{H}$ are maximal monotone operators and that A is σ -strongly monotone and β -Lipschitz continuous. Then the parameters that optimize the rate in (10) are given by $\theta = 1$ and $\gamma = \frac{1}{\beta}$. Further, the optimal rate becomes $\sqrt{1 - \frac{\sigma}{\beta}}$.

Proof. It is straightforward to verify that the expression $|1 - \alpha| + \alpha\sqrt{1 - \frac{4\gamma\sigma}{(1+\gamma\beta)^2}}$ is decreasing in α for $\alpha \leq 1$ and increasing in α for $\alpha \geq 1$ for any choice of $\gamma > 0$. Hence, $\alpha = 1$ optimizes the rate. The optimal γ is obtained by minimizing $\frac{4\gamma\sigma}{(1+\gamma\beta)^2}$ w.r.t. γ . Differentiation gives

$$\frac{4\sigma}{(1+\gamma\beta)^2} - \frac{8\sigma\gamma\beta}{(1+\gamma\beta)^3} = 0$$

which implies $\gamma = \pm 1/\beta$. Since $\gamma > 0$, we have $\gamma = 1/\beta$. Inserting these into the rate factor $\left(1 - \alpha\left(1 - \sqrt{1 - \frac{4\gamma\sigma}{(1+\gamma\beta)^2}}\right)\right)$ gives the optimal rate factor $\sqrt{1 - \frac{\sigma}{\beta}}$. \square

When we restrict ourselves to solve inclusion problems of the form (5) for maximal monotone operators $A = \partial f$ and $B = \partial g$, where $f \in \Gamma_0(\mathcal{H})$ and $g \in \Gamma_0(\mathcal{H})$, these complexity bounds can be significantly improved. Finding a point x that solves the inclusion

$$0 \in \partial f(x) + \partial g(x)$$

is equivalent to solving the following composite convex optimization problem

$$\text{minimize } f(x) + g(x). \quad (11)$$

This implies that generalized Douglas-Rachford splitting can be applied to solve composite optimization problems. In the following theorem, we present the improved linear convergence rate results for generalized Douglas-Rachford splitting in the context of composite convex optimization.

Theorem 1: Suppose that $f, g \in \Gamma_0(\mathcal{H})$ and that f is σ -strongly convex and β -smooth. Then the generalized Douglas-Rachford algorithm (6) converges linearly towards a $\bar{z} \in \text{fix}(R_{\gamma f} R_{\gamma g})$ with rate $|1 - \alpha| + \alpha \max\left(\frac{\gamma\beta-1}{\gamma\beta+1}, \frac{1-\gamma\sigma}{1+\gamma\sigma}\right)$, i.e.

$$\|z^{k+1} - \bar{z}\| \leq \left(|1 - \alpha| + \alpha \max\left(\frac{\gamma\beta-1}{\gamma\beta+1}, \frac{1-\gamma\sigma}{1+\gamma\sigma}\right)\right)^k \|z^0 - \bar{z}\|.$$

Proof. The proof is almost identical to the proof to Proposition 14 in Appendix C. The only difference is that the contraction factor δ of $R_{\gamma f}$ should be $\max\left(\frac{\gamma\beta-1}{\gamma\beta+1}, \frac{1-\gamma\sigma}{1+\gamma\sigma}\right)$ instead, according to Proposition 13. \square

Also in this case, the parameter α can be chosen greater than 1. Similarly to in Remark 1, we get for $\alpha > 1$ that

$$\begin{aligned} |1 - \alpha| + \alpha \max\left(\frac{\gamma\beta-1}{\gamma\beta+1}, \frac{1-\gamma\sigma}{1+\gamma\sigma}\right) &< 1 \\ \Leftrightarrow \alpha &< \frac{2}{1 + \max\left(\frac{\gamma\beta-1}{\gamma\beta+1}, \frac{1-\gamma\sigma}{1+\gamma\sigma}\right)}. \end{aligned} \quad (12)$$

Again, the parameters γ and α can be chosen to optimize the bound on the convergence rate. This is done in the following proposition.

Proposition 16: Suppose that $f, g \in \Gamma_0(\mathcal{H})$ and that f is σ -strongly convex and β -smooth. Then the optimal parameters for the generalized Douglas-Rachford algorithm are given by $\alpha = 1$ and $\gamma = \frac{1}{\sqrt{\sigma\beta}}$ and the optimal rate is given by $\frac{\sqrt{\beta/\sigma-1}}{\sqrt{\beta/\sigma+1}}$.

Proof. It is straightforward to verify that $|1 - \alpha| + \alpha \max\left(\frac{\gamma\beta-1}{\gamma\beta+1}, \frac{1-\gamma\sigma}{1+\gamma\sigma}\right)$ is a decreasing function of α for $\alpha \leq 1$ and increasing for $\alpha \geq 1$. Therefore the rate factor is optimized by $\alpha = 1$. The γ parameter should be chosen to minimize the max-expression $\max\left(\frac{\gamma\beta-1}{\gamma\beta+1}, \frac{1-\gamma\sigma}{1+\gamma\sigma}\right)$. This is done by setting the arguments equal, which gives $\gamma = 1/\sqrt{\sigma\beta}$. Inserting these values into the rate factor expression gives $\frac{\sqrt{\beta/\sigma-1}}{\sqrt{\beta/\sigma+1}}$. \square

Note that in Propositions 15 and 16, $\alpha = 1$ is optimal. That is, the Peaceman-Rachford algorithm gives the fastest convergence rate under the strong monotonicity and Lipschitz continuity assumptions, even though the Peaceman-Rachford algorithm is not guaranteed to converge in the general case.

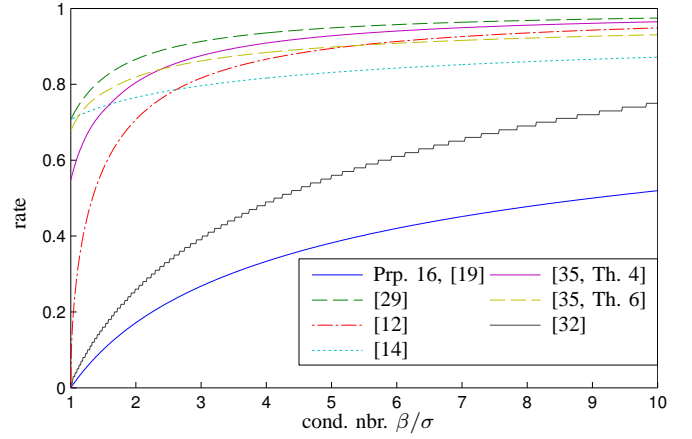


Fig. 4. Comparison between bounds on the linear convergence rate for Douglas-Rachford splitting provided in [12], [14], [19], [35], [29] and in Proposition 16 for different conditioning of the data. Proposition 16 provides the tightest bound on the rate for all ratios β/σ .

B. Comparison to other methods

In this section, we discuss in what ways our result in Proposition 16 generalizes and/or improves on previously known linear convergence rate results in [12], [14], [19], [35], [29] and the linear convergence rate [32] that appeared online during the submission procedure of this paper. Since Douglas-Rachford splitting and ADMM are equivalent in the case where $\mathcal{A} = \text{Id}$ (that is, Douglas-Rachford is self-dual, i.e., it gives equivalent algorithms if applied to the primal and the dual when $\mathcal{A} = \text{Id}$) we can compare DR convergence rate results with ADMM convergence rate results by letting $\mathcal{A} = \text{Id}$. The underlying assumption for all rate bounds in this comparison is that one of the two maximal monotone operators in the inclusion problem (5) is σ -strongly monotone and β -Lipschitz continuous. Some results hold for problems with general maximal monotone operators, while other results holds for the restricted class of composite convex optimization.

In [29, Proposition 4, Remark 10], the linear convergence rate for Douglas-Rachford splitting, i.e. (6) with $\alpha = \frac{1}{2}$, when solving the general inclusion problem (5) is shown to be $\sqrt{1 - \frac{2\gamma\sigma}{(1+\gamma\beta)^2}}$. This rate is optimized by $\gamma = 1/\beta$, which gives a rate of $\sqrt{1 - \frac{2\sigma}{\beta}}$. This was generalized, in the setting of the operators being subdifferentials to proper, closed, and convex functions, to any α in [12, Theorem 6]. The rate in [12, Theorem 6] is $\sqrt{1 - \frac{4\alpha\gamma\sigma}{(1+\gamma\beta)^2}}$. The optimal parameters are $\alpha = 1$ and $\gamma = 1/\beta$, and the optimal rate becomes $\sqrt{1 - \frac{\sigma}{\beta}}$. It can be shown that the result in Proposition 15 is a slight improvement (except for the case $\alpha = 1$ when the estimates coincide) to the result in [12, Theorem 6]. Proposition 15 is also a generalization since it holds for general maximal monotone operators and for a wider range of α values. Compared to Proposition 16, we see in Figure 4 that Proposition 16 gives a better bound than [12, Theorem 6] for all ratios β/σ .

The optimal convergence rate in [14, Corollary 3.6] is given by $\sqrt{1/(1 + 1/\sqrt{\beta/\sigma})}$, and the optimal parameter coincides

with our choice in Proposition 16. Figure 4 shows that the convergence rate bound in Proposition 16 is tighter than the one provided in [14, Corollary 3.6] for all values of the ratio β/σ . Proposition 16 also generalizes [14, Corollary 3.6] since [14, Corollary 3.6] is stated in the Euclidean setting.

In [35], a new interpretation to Douglas-Rachford splitting is presented. They show that if γ is small enough ($\gamma < 1/\beta$) and if f is a quadratic, then the Douglas-Rachford splitting is equivalent to a gradient method applied to a function named the Douglas-Rachford envelope. The Lipschitz continuity and strong convexity parameters for the envelope function can be computed from the corresponding values of the original function f . Convergence rate estimates follow from the convergence results for the gradient method. Since the Douglas-Rachford envelope is smooth, they also propose an accelerated Douglas-Rachford algorithm (under the same assumptions, i.e., f quadratic and $\gamma < 1/\beta$). The convergence rate estimates of this also follow from the convergence rate estimates of fast gradient methods. In Figure 4, we plot the convergence rate estimates for the standard Douglas-Rachford algorithm [35, Theorem 4] and the fast Douglas-Rachford algorithm in [35, Theorem 6], both with parameter $\gamma = (\sqrt{2} - 1)/\beta$. We see that Proposition 16 gives better rates for all values of the ratio β/σ . Proposition 16 is also more general in applicability.

The results provided in [19] coincide with the results provided in Proposition 16. However, the generality of our analysis makes Proposition 16 applicable to a much wider class of problems than the finite-dimensional quadratic problems with linear inequality constraints considered in [19].

Finally, we compare our rate bound to the rate bound in [32]. Figure 4 shows that our bound is indeed tighter for all values of the ratio β/σ . As opposed to all the other rate bounds in this comparison, the rate bound in [32] is not explicit. Rather, a sweep over different rate bound factors are needed. For each guess, a small semi-definite program is solved to assess whether the algorithm is guaranteed to converge with that rate. This is also the cause of the steps in the plot in Figure 4, where the size of the steps are due to the quantization levels of our sweep.

Besides generalizing and/or improving on existing results, the results in Proposition 16 can guide us in choosing a space on which to perform the Douglas-Rachford algorithm when solving finite-dimensional problems. By selecting the space appropriately, this can significantly improve the convergence properties of the algorithm, both in theory and in practice. This is the topic of the following section.

C. Metric selection

In this section, we consider finite-dimensional composite convex optimization problems of the form (11), where f and g satisfy:

Assumption 1:

- (i) The function $f \in \Gamma_0(\mathbb{H}_M)$ is 1-strongly convex if defined on \mathbb{H}_H and 1-smooth if defined on \mathbb{H}_L .
- (ii) The function $g \in \Gamma_0(\mathbb{H}_M)$.

Examples of functions f that satisfy Assumption 1(i) are piece-wise quadratic functions with Hessians Q_i that are

differentiable on the boundary between the regions. The matrix H satisfies $0 \prec H \preceq Q_i$ for all i and L satisfies $L \succeq Q_i$ for all i . Obviously, in the general case we have $L \succeq H$ and for a standard quadratic function with Hessian H , we have $L = H$. Depending on which space \mathbb{H}_M we define the functions f and g we will get different algorithms and different convergence properties. Proposition 16 suggests that we should select a space \mathbb{H}_M on which the ratio β/σ is as small as possible, i.e., on which the conditioning of the function f is as good as possible. Next, we present a result that shows how β and σ varies with M under Assumption 1.

Proposition 17: Suppose that $f \in \Gamma_0(\mathbb{H}_M)$ satisfies Assumption 1(i) and that $M = (D^T D)^{-1}$. Then the strong convexity modulus $\sigma_M(f)$ and the smoothness parameter $\beta_M(f)$ are given by

$$\begin{aligned}\beta_M(f) &= \lambda_{\max}(DLD^T) \\ \sigma_M(f) &= \lambda_{\min}(DHD^T).\end{aligned}$$

Proof. Denote by $\nabla_M f$ the gradient of f when defined on \mathbb{H}_M and $\nabla_2 f$ the gradient of f when defined on \mathbb{R}^n . Then $\nabla_M f = M^{-1} \nabla_2 f$ since

$$\begin{aligned}f(x) &\geq f(y) + \langle \nabla_M f(x), x - y \rangle_M \\ \Leftrightarrow f(x) &\geq f(y) + \langle M \nabla_M f(x), x - y \rangle_2\end{aligned}$$

where $M \nabla_M f = \nabla_2 f$. Therefore,

$$\begin{aligned}\langle \nabla f(x) - \nabla f(y), x - y \rangle_{M_1} &= \langle \nabla f(x) - \nabla f(y), x - y \rangle_{M_2} \\ \|\nabla f(x) - \nabla f(y)\|_{M_1} &= \|\nabla f(x) - \nabla f(y)\|_{M_2}\end{aligned}$$

for any $M_1, M_2 \succ 0$. Further, by letting $M_2 = (D_2^T D_2)^{-1}$, we have

$$\begin{aligned}\|x\|_{M_1} &\geq \lambda_{\min}(D_2 M_1 D_2^T) \|x\|_{M_2} \\ \|x\|_{M_1} &\leq \lambda_{\max}(D_2 M_1 D_2^T) \|x\|_{M_2}.\end{aligned}$$

The first inequality holds since

$$\begin{aligned}\|x\|_{M_1} &\geq \lambda_{\min}(D_2 M_1 D_2^T) \|x\|_{M_2} \\ \Leftrightarrow \|D_2^T x\|_{M_1} &\geq \lambda_{\min}(D_2 M_1 D_2^T) \|D_2^T x\|_{M_2} \\ \Leftrightarrow \|x\|_{D_2 M_1 D_2^T} &\geq \lambda_{\min}(D_2 M_1 D_2^T) \|x\|_2 \\ \Leftrightarrow D_2 M_1 D_2^T &\succeq \lambda_{\min}(D_2 M_1 D_2^T) I.\end{aligned}$$

The second inequality is proven similarly. Since f is 1-strongly convex if defined on \mathbb{H}_H , we get

$$\begin{aligned}\langle \nabla f(x) - \nabla f(y), x - y \rangle_M &= \langle \nabla f(x) - \nabla f(y), x - y \rangle_H \\ &\geq \|x - y\|_H^2 \geq \lambda_{\min}(DHD^T) \|x - y\|_M^2.\end{aligned}$$

That is, $\sigma_M(f) = \lambda_{\min}(DHD^T)$. Further, since f is 1-smooth if defined on \mathbb{H}_L , we get

$$\begin{aligned}\|\nabla f(x) - \nabla f(y)\|_M &= \|\nabla f(x) - \nabla f(y)\|_L \\ &\leq \|x - y\|_L \leq \lambda_{\max}(DLD^T) \|x - y\|_M^2.\end{aligned}$$

Thus, $\beta_M(f) = \lambda_{\max}(DLD^T)$ and the proof is complete. \square

This result indicates that, to optimize the rate in Proposition 16, we should select a metric $M = (D^T D)^{-1}$ that solves

$$\text{minimize } \frac{\beta_M(f)}{\sigma_M(f)} = \text{minimize } \frac{\lambda_{\max}(DLD^T)}{\lambda_{\min}(DHD^T)}. \quad (13)$$

In accordance with Proposition 16, the algorithm parameter γ should be chosen as $\gamma = \frac{1}{\sqrt{\lambda_{\max}(DLD^T)\lambda_{\min}(DHD^T)}}$. To select a metric according to (13) can significantly improve the convergence rate bound compared to applying the algorithm in the standard Euclidean space. This is suggested by the following example. Suppose that we minimize a problem with a quadratic function f with Hessian H , and run the generalized Douglas-Rachford algorithm on the Euclidean space with $M = D = I$. Then Proposition 16 guarantees the rate $\frac{\sqrt{\lambda_{\max}(H)/\lambda_{\min}(H)-1}}{\sqrt{\lambda_{\max}(H)/\lambda_{\min}(H)+1}}$. If we instead apply the generalized Douglas-Rachford algorithm on \mathbb{H}_M with $M = H$ and $D = H^{-1/2}$ (which optimizes (13)), we get rate $\frac{\sqrt{\lambda_{\max}(H^{-1/2}HH^{-1/2})/\lambda_{\min}(H^{-1/2}HH^{-1/2})-1}}{\sqrt{\lambda_{\max}(H^{-1/2}HH^{-1/2})/\lambda_{\min}(H^{-1/2}HH^{-1/2})+1}} = 0$. That is, we get super-linear convergence. The more ill-conditioned the original problem is, the more we improve the rate bound by selecting a better metric for the problem. However, often the functions f and/or g are separable down to the component. In such cases, choosing a non-diagonal M would significantly increase the computational complexity when evaluating the prox-operator. Therefore, to get an efficient algorithm both in terms of convergence rate and in terms of complexity within each iteration, the metric matrix $M = (D^T D)^{-1}$ should be chosen to minimize (13), subject to M being diagonal. In [21, Section 6] methods to minimize (13) exactly as well as computationally cheap methods to reduce the ratio in (13) are presented.

D. Preconditioning

To apply the Douglas-Rachford algorithm on the space \mathbb{H}_M is equivalent to apply Douglas-Rachford splitting on the Euclidean space \mathbf{R}^n to the preconditioned problem

$$\text{minimize } f_D(x) + g_D(x) \quad (14)$$

where $M = (D^T D)^{-1}$ and

$$\begin{aligned} f_D(x) &:= f(D^T x) \\ g_D(x) &:= g(D^T x) \end{aligned}$$

and $f, f_D, g,$ and g_D are defined on the Euclidean space \mathbf{R}^n . This can be seen as follows. Let $\{x_{\text{pc}}^k\}, \{y_{\text{pc}}^k\},$ and $\{z_{\text{pc}}^k\}$ be the Douglas-Rachford iterates (7)-(9) when solving the preconditioned problem (14) on \mathbf{R}^n and let $\{x_M^k\}, \{y_M^k\},$ and $\{z_M^k\}$ be the Douglas-Rachford iterates (7)-(9) when solving the original problem on \mathbb{H}_M . Further assume that $z_{\text{pc}}^0 = D^{-T} z_M^0$. Then, using notation $f_{\mathbb{H}_M}$ and $g_{\mathbb{H}_M}$ when

functions f and g are defined on \mathbb{H}_M , we get

$$\begin{aligned} x_{\text{pc}}^0 &= \text{prox}_{\gamma f_D}(z_{\text{pc}}^0) = \underset{x}{\text{argmin}} \left\{ f_D(x) + \frac{1}{2\gamma} \|x - z_{\text{pc}}^0\|^2 \right\} \\ &= D^{-T} \underset{v}{\text{argmin}} \left\{ f(v) + \frac{1}{2\gamma} \|D^{-T}v - z_{\text{pc}}^0\|^2 \right\} \\ &= D^{-T} \underset{v}{\text{argmin}} \left\{ f(v) + \frac{1}{2\gamma} \|v - D^T z_{\text{pc}}^0\|_{D^T D}^2 \right\} \\ &= D^{-T} \underset{v}{\text{argmin}} \left\{ f_{\mathbb{H}_M}(v) + \frac{1}{2\gamma} \|v - z_M^0\|^2 \right\} \\ &= D^{-T} \text{prox}_{\gamma f_{\mathbb{H}_M}}(z_M^0) = D^{-T} x_M^0. \end{aligned}$$

The same thing can be shown for the y -updates, i.e., that $y_{\text{pc}}^0 = D^{-T} y_M^0$. Finally,

$$\begin{aligned} z_{\text{pc}}^1 &= z_{\text{pc}}^0 + 2\theta(y_{\text{pc}}^0 - x_{\text{pc}}^0) \\ &= D^{-T}(z_M^0 + 2\theta(y_M^0 - x_M^0)) = D^{-T} z_M^1. \end{aligned}$$

Recursive application of these statements shows the equivalence.

The conceptual difference between the Douglas-Rachford algorithm applied on \mathbb{H}_M to solve the original problem, and the Douglas-Rachford algorithm applied on \mathbf{R}^n to solve the preconditioned problem, is that in the former case, the metric in the algorithm is chosen to fit the problem data, while in the second case, the problem data is preconditioned to fit the fixed algorithm metric.

V. ADMM

In this section, besides \mathcal{H} being a real Hilbert space, also \mathcal{K} denotes a real Hilbert space. Here, we consider solving problems of the form

$$\text{minimize } f(x) + g(\mathcal{A}x) \quad (15)$$

that satisfy the following assumptions:

Assumption 2:

- (i) The function $f \in \Gamma_0(\mathcal{H})$ is β -smooth and σ -strongly convex.
- (ii) The function $g \in \Gamma_0(\mathcal{K})$.
- (iii) The bounded linear operator $\mathcal{A} : \mathcal{H} \rightarrow \mathcal{K}$ is surjective.

The assumption of \mathcal{A} being a surjective bounded linear operator reduces to \mathcal{A} being a real matrix with full row rank in the Euclidean case. Problems of the form (15) cannot be directly efficiently solved using generalized Douglas-Rachford splitting. Therefore, we instead solve the (negative) Fenchel dual problem, which is given by (see [3, Definition 15.19])

$$\text{minimize } d(\mu) + g^*(\mu) \quad (16)$$

where $g^* \in \Gamma_0(\mathcal{K})$ and $d \in \Gamma_0(\mathcal{K})$ is

$$d(\mu) := f^*(-\mathcal{A}^* \mu) \quad (17)$$

where $\mathcal{A}^* : \mathcal{K} \rightarrow \mathcal{H}$ is the adjoint operator of \mathcal{A} , defined as the unique operator that satisfies $\langle \mathcal{A}x, \mu \rangle = \langle x, \mathcal{A}^* \mu \rangle$ for all $x \in \mathcal{H}$ and $\mu \in \mathcal{K}$. Applying Douglas-Rachford splitting (i.e. generalized Douglas-Rachford splitting with $\alpha = \frac{1}{2}$) to the dual is well known to be equivalent to applying ADMM to the primal, see [17], [16]. To apply generalized Douglas-Rachford splitting to the dual for other choices of α is known

as ADMM with over-relaxation for $\alpha \in (\frac{1}{2}, 1]$ and ADMM with under-relaxation for $\alpha \in (0, \frac{1}{2})$ (here we show that also $\alpha > 1$ is possible under Assumption 2). Therefore, the results we obtain in this section applies to relaxed ADMM.

A. Linear convergence

To optimize the bound on the linear convergence rate in Proposition 16 when applied to solve the dual problem (16), we need to quantify the strong convexity and smoothness parameters for d . This is done in the following proposition.

Proposition 18: Suppose that Assumption 2 holds. Then $d \in \Gamma_0(\mathcal{K})$ is $\frac{\|\mathcal{A}^*\|^2}{\sigma}$ -smooth and $\frac{\theta^2}{\beta}$ -strongly convex, where $\theta > 0$ always exists and satisfies $\|\mathcal{A}^*\mu\| \geq \theta\|\mu\|$ for all $\mu \in \mathcal{K}$.

Proof. Since f is σ -strongly convex, Proposition 4 gives that f^* is $\frac{1}{\sigma}$ -smooth. Therefore, d satisfies

$$\begin{aligned} \|\nabla d(\mu) - \nabla d(\nu)\| &= \|\mathcal{A}\nabla f^*(-\mathcal{A}^*\mu) - \mathcal{A}\nabla f^*(-\mathcal{A}^*\nu)\| \\ &\leq \frac{\|\mathcal{A}\|}{\sigma} \|\mathcal{A}^*(\mu - \nu)\| \\ &\leq \frac{\|\mathcal{A}^*\|^2}{\sigma} \|\mu - \nu\| \end{aligned}$$

since $\|\mathcal{A}\| = \|\mathcal{A}^*\|$. This is equivalent to that d is $\frac{\|\mathcal{A}^*\|^2}{\sigma}$ -smooth, see Proposition 4.

Next, we show the strong convexity result. The property that f is β -smooth implies through Proposition 4 that f^* is $\frac{1}{\beta}$ -strongly convex. This implies that d satisfies

$$\begin{aligned} \langle \nabla d(\mu) - \nabla d(\nu), \mu - \nu \rangle &= \langle -\mathcal{A}(\nabla f^*(-\mathcal{A}^*\mu) - \nabla f^*(-\mathcal{A}^*\nu)), \mu - \nu \rangle \\ &= \langle \nabla f^*(-\mathcal{A}^*\mu) - \nabla f^*(-\mathcal{A}^*\nu), -\mathcal{A}^*\mu + \mathcal{A}^*\nu \rangle \\ &\geq \frac{1}{\beta} \|\mathcal{A}^*(\mu - \nu)\|^2 \geq \frac{\theta^2}{\beta} \|\mu - \nu\|^2. \end{aligned}$$

which by Proposition 4 is equivalent to d being $\frac{\theta^2}{\beta}$ -strongly convex. That $\theta > 0$ follows from [3, Fact 2.18 and Fact 2.19]. Specifically, Fact 2.18 says that $\ker \mathcal{A}^* = (\text{ran} \mathcal{A})^\perp = \emptyset$, since A is surjective. Since $\text{ran} \mathcal{A} = \mathcal{K}$ (again by surjectivity), it is closed. Then Fact 2.19 states that there exists $\theta > 0$ such that $\|\mathcal{A}^*\mu\| \geq \theta\|\mu\|$ for all $\mu \in (\ker \mathcal{A}^*)^\perp = (\emptyset)^\perp = \mathcal{K}$. This concludes the proof. \square

This result gives us the following immediate corollary.

Corollary 2: Suppose that Assumption 2 holds and that generalized Douglas-Rachford is applied to solve the dual problem (16) (or equivalently ADMM is applied to solve the primal (15)). Then the algorithm converges at least with the rate $|1 - \alpha| + \alpha \max\left(\frac{\gamma\hat{\beta}-1}{1+\gamma\hat{\beta}}, \frac{1-\gamma\hat{\sigma}}{1+\gamma\hat{\sigma}}\right)$ where $\hat{\beta} = \frac{\|\mathcal{A}^*\|^2}{\sigma}$ and $\hat{\sigma} = \frac{\theta^2}{\beta}$. Further, the algorithm parameters γ and α that optimize the rate bound are $\alpha = 1$ and $\gamma = \frac{1}{\sqrt{\beta\hat{\sigma}}} = \frac{\sqrt{\beta\sigma}}{\sqrt{\|\mathcal{A}^*\|^2\theta^2}}$. The optimized linear convergence rate bound factor is $\frac{\sqrt{\kappa-1}}{\sqrt{\kappa+1}}$, where $\kappa = \frac{\hat{\beta}}{\hat{\sigma}} = \frac{\|\mathcal{A}^*\|^2\beta}{\theta^2\sigma}$.

Proof. This follows directly from Propositions 18 and 16 and Theorem 1. \square

Remark 2: Also in the dual case, the α -parameter can be chosen greater than one. The upper bound on α is given in (12) with β and σ replaced by $\hat{\beta} = \frac{\|\mathcal{A}^*\|^2}{\sigma}$ and $\hat{\sigma} = \frac{\theta^2}{\beta}$ respectively.

The convergence rate bounds in Corollary 2 depend both on the conditioning of the function f and the conditioning of the linear operator \mathcal{A}^* . The better the conditioning, the faster the rate. However, some of the parameters might be hard to compute or estimate, especially θ . In the following section, we show how to compute this in finite-dimensional Hilbert spaces \mathbb{H}_K . We also show how to select the space \mathbb{H}_K (i.e., select matrix K) to optimize the bound on the convergence rate.

B. Metric selection

In this section, we still consider problems of the form (15) and we suppose that the following assumptions hold:

Assumption 3:

- (i) The function $f \in \Gamma_0(\mathbb{H}_M)$ is 1-strongly convex if defined on \mathbb{H}_H and 1-smooth if defined on \mathbb{H}_L .
- (ii) The function $g \in \Gamma_0(\mathbb{H}_K)$.
- (iii) The bounded linear operator $\mathcal{A} : \mathbb{H}_H \rightarrow \mathbb{H}_K$ is surjective.

Items (i) and (ii) are the same as in Assumption 1, and the assumption on the bounded linear operator is added due to the more general problem formulation treated here.

Also here, we solve (15) by applying Douglas-Rachford splitting on the dual problem (16), or equivalently by applying ADMM directly on the primal (15). In this case, we have the possibility to select the space \mathbb{H}_K on which to define the dual problem and apply the algorithm. To aid in the selection of such a space, we show in the following proposition how the strong convexity modulus and smoothness constant of $d \in \Gamma_0(\mathbb{H}_K)$ depend on the space on which it is defined.

Proposition 19: Suppose that Assumption 3 holds, that $A \in \mathbf{R}^{m \times n}$ satisfies $Ax = \mathcal{A}x$ for all x , and that $K = E^T E$. Then $d \in \mathbb{H}_K$ is $\|EAH^{-1}A^T E^T\|$ -smooth and $\lambda_{\min}(EAL^{-1}A^T E^T)$ -strongly convex, where $\lambda_{\min}(EAL^{-1}A^T E^T) > 0$.

Proof. First, we relate $\mathcal{A}^* : \mathbb{H}_K \rightarrow \mathbb{H}_M$ to A , M (f is defined on \mathbb{H}_M), and K . We have

$$\begin{aligned} \langle Ax, \mu \rangle_K &= \langle Ax, K\mu \rangle_2 = \langle x, A^T K\mu \rangle_2 = \langle x, H^{-1}A^T K\mu \rangle_H \\ &= \langle H^{-1}A^T K\mu, x \rangle_H = \langle \mathcal{A}^*\mu, x \rangle_H. \end{aligned}$$

Thus, $\mathcal{A}^*\mu = H^{-1}A^T K\mu$ for all $\mu \in \mathbb{H}_K$.

Next, we show that the space \mathbb{H}_M on which f (and f^*) is defined does not influence the shape of d . Denote by $d_H := f_H^* \circ -\mathcal{A}_H^*$ where f_H is defined on \mathbb{H}_H and $\mathcal{A}_H^* : \mathbb{H}_K \rightarrow \mathbb{H}_H$, by $d_L := f_L^* \circ -\mathcal{A}_L^*$ where f_L is defined on \mathbb{H}_L and $\mathcal{A}_L^* : \mathbb{H}_K \rightarrow \mathbb{H}_L$, and by $d_e := f_e^* \circ -A^T$, where f_e^* and A are defined on the Euclidean space. By these definitions both d_L and d_H are defined on \mathbb{H}_K , while d_e is defined on \mathbf{R}^m . Next we show that d_L and d_H are identical for any μ :

$$\begin{aligned} d_H(\mu) &= f_H^*(-\mathcal{A}_H^*\mu) = \sup_x \{ \langle -\mathcal{A}_H^*\mu, x \rangle_H - f_H(x) \} \\ &= \sup_x \{ \langle -HH^{-1}A^T K\mu, x \rangle_2 - f_e(x) \} \\ &= \sup_x \{ \langle -LL^{-1}A^T K\mu, x \rangle_2 - f_e(x) \} \\ &= \sup_x \{ \langle -\mathcal{A}_L^*\mu, x \rangle_L - f_L(x) \} = d_L(\mu) \end{aligned}$$

where $\mathcal{A}_H^* \mu = H^{-1} A^T K \mu$ is used. This implies that we can show properties of $d \in \mathbb{H}_K$ by defining f on any space \mathbb{H}_M .

Thus, Proposition 18 gives that 1-strong convexity of f when defined on \mathbb{H}_H implies $\|\mathcal{A}^*\|^2$ -smoothness of d , where

$$\begin{aligned} \|\mathcal{A}^*\| &= \sup_{\mu} \{ \|\mathcal{A}^* \mu\| \mid \|\mu\| \leq 1 \} \\ &= \sup_{\mu} \{ \|H^{-1} A^T K \mu\|_H \mid \|\mu\|_K \leq 1 \} \\ &= \sup_{\mu} \left\{ \|H^{-1/2} A^T E^T E \mu\|_2 \mid \|E \mu\|_2 \leq 1 \right\} \\ &= \sup_{\nu} \left\{ \|H^{-1/2} A^T E^T \nu\|_2 \mid \|\nu\|_2 \leq 1 \right\} \\ &= \|H^{-1/2} A^T E^T\|_2. \end{aligned}$$

To show the strong-convexity claim, we use that 1-smoothness of f when defined on \mathbb{H}_L implies θ^2 -strong convexity of d where $\theta > 0$ satisfies $\|\mathcal{A}^* \mu\| \geq \theta \|\mu\|$ for all $\mu \in \mathbb{H}_K$, see Proposition 18. Such a θ is given by

$$\begin{aligned} \|\mathcal{A}^* \mu\|_L^2 &= \|L^{-1} A^T K \mu\|_L^2 = \|L^{-1/2} A^T E^T (E \mu)\|_2^2 \\ &= \|E \mu\|_{EAL^{-1}A^TE^T}^2 \\ &\geq \lambda_{\min}(EAL^{-1}A^TE^T) \|E \mu\|_2^2 \\ &= \lambda_{\min}(EAL^{-1}A^TE^T) \|\mu\|_K^2. \end{aligned}$$

The smallest eigenvalue $\lambda_{\min}(EAL^{-1}A^TE^T) > 0$ since A is surjective, i.e. has full row rank, and E and L are positive definite matrices. This concludes the proof. \square

This result shows how the Lipschitz constant and strong convexity modulus of $d \in \Gamma_0(\mathbb{H}_K)$ changes with the space \mathbb{H}_K on which it is defined. Combining this with Proposition 16, we get that the bound on the convergence rate for Douglas-Rachford splitting applied to the dual problem (16), or equivalently ADMM applied to the primal (15), is optimized by choosing $K = E^T E$ where E solves

$$\text{minimize} \quad \frac{\lambda_{\max}(EAH^{-1}A^TE^T)}{\lambda_{\min}(EAL^{-1}A^TE^T)} \quad (18)$$

and by choosing $\gamma = \frac{1}{\sqrt{\lambda_{\max}(EAH^{-1}A^TE^T)\lambda_{\min}(EAL^{-1}A^TE^T)}}$. As for Douglas-Rachford splitting applied to the primal problem, using a non-diagonal K usually gives prohibitively expensive prox-evaluations. Therefore, we propose to select a diagonal $K = E^T E$ that minimizes (18). The reader is referred to [21, Section 6] for different methods to achieve this exactly and approximately.

The procedure of selecting the metric for the dual Douglas-Rachford splitting is slightly different compared to the primal version. In the primal, we assume that we are given matrices H and L that define spaces \mathbb{H}_H and \mathbb{H}_L on which the function f is 1-strongly convex and 1-smooth respectively. To get optimal convergence behaviour, we suppose that these matrices are as tight as possible. Then a diagonal metric M (that defines \mathbb{H}_M on which the problem is defined) is chosen that optimizes the bound on the convergence rate. This metric affects only the algorithm, while the problem is the same for any choice of metric matrix M .

In the dual formulation, we are not given matrices on which the dual is β -strongly convex and σ -smooth respectively. Tight

estimates of these parameters are instead computed and we show how these depend on the space \mathbb{H}_K on which the dual problem is defined. Since the dual problem actually changes with the space on which it is defined, the choice of \mathbb{H}_K affects both the shape of the dual problem and the metric used in the algorithm. Therefore, the interpretation made for the primal that the algorithm metric is chosen to well estimate the level-sets of problem is not exactly true in this case. When we select a space \mathbb{H}_K for the dual, instead we simultaneously manipulate the level-sets of the dual problem and the metric in the algorithm such that the metric well approximates the manipulated level sets of the function d .

C. Preconditioning

Similarly to in the primal Douglas-Rachford case, it is equivalent to apply Douglas-Rachford splitting on the dual problem on the space \mathbb{H}_K and to solve the following preconditioned dual problem defined on the Euclidean space:

$$\text{minimize} \quad d_E(\nu) + g_E^*(\nu) \quad (19)$$

where $K = E^T E$,

$$\begin{aligned} d_E(\nu) &:= d(E^T \nu) \\ g_E^*(\nu) &:= g^*(E^T \nu), \end{aligned}$$

and d , d_E , g^* , and g_E^* are defined on the Euclidean space \mathbf{R}^m . To distinguish on which space f and g are defined, we denote the functions d and g^* by $d_{\mathbb{H}_K}$ and $g_{\mathbb{H}_K}^*$ respectively when defined on \mathbb{H}_K . We will also need the equality $d_{\mathbb{H}_K}(\mu) = d(K\mu)$ and $g_{\mathbb{H}_K}^*(\mu) = d(K\mu)$ which holds since

$$\begin{aligned} d_{\mathbb{H}_K}(\mu) &= f_{\mathbb{H}_H}^*(-\mathcal{A}^* \mu) \\ &= \sup_x \{ \langle -\mathcal{A}^* \mu, x \rangle_H - f_{\mathbb{H}_H}(x) \} \\ &= \sup_x \{ \langle -HH^{-1}A^TK\mu, x \rangle_2 - f(x) \} \\ &= \sup_x \{ \langle -A^TK\mu, x \rangle_2 - f(x) \} \\ &= f^*(-A^TK\mu) = d(K\mu) \end{aligned}$$

where $\mathcal{A}^* \mu = H^{-1} A^T K \mu$ has been used.

To see the equivalence, we let $\{x_{\text{pc}}^k\}$, $\{y_{\text{pc}}^k\}$, and $\{z_{\text{pc}}^k\}$ be the Douglas-Rachford iterates (7)-(9) when solving the preconditioned problem (19) on \mathbf{R}^n and let $\{x_K^k\}$, $\{y_K^k\}$, and $\{z_K^k\}$ be the Douglas-Rachford iterates (7)-(9) when solving the original dual problem (16) on \mathbb{H}_K . Further assume that $Ez_{\text{pc}}^0 = z_K^0$. Then

$$\begin{aligned} x_{\text{pc}}^0 &= \text{prox}_{\gamma d_{\mathbb{H}_K}}(z_{\text{pc}}^0) = \underset{\mu}{\text{argmin}} \left\{ d_{\mathbb{H}_K}(\mu) + \frac{1}{2\gamma} \|x - z_{\text{pc}}^0\|^2 \right\} \\ &= \underset{\mu}{\text{argmin}} \left\{ d(K\mu) + \frac{1}{2\gamma} \|x - z_{\text{pc}}^0\|_K^2 \right\} \\ &= E^{-1} \underset{\nu}{\text{argmin}} \left\{ d(E^T \nu) + \frac{1}{2\gamma} \|\nu - Ez_{\text{pc}}^0\|_2^2 \right\} \\ &= E^{-1} \text{prox}_{\gamma d_E}(z_K^0) = E^{-1} x_K^0 \end{aligned}$$

The same thing can be shown for the y -updates, i.e., that $y_{\text{pc}}^0 = E^{-1} y_M^0$. Finally,

$$\begin{aligned} z_{\text{pc}}^1 &= z_{\text{pc}}^0 + 2\theta(y_{\text{pc}}^0 - x_{\text{pc}}^0) \\ &= E^{-1}(z_K^0 + 2\theta(y_K^0 - x_K^0)) = E^{-1} z_K^1. \end{aligned}$$

Recursive application of these statements shows the equivalence.

The primal problem that gives rise to the preconditioned dual problem (19) is given by

$$\begin{aligned} & \text{minimize} && f(x) + g(y) \\ & \text{subject to} && EAx = Ey. \end{aligned} \quad (20)$$

Since solving the problem (19) using generalized Douglas-Rachford splitting is equivalent to solving the primal problem (20) using ADMM, the result presented for dual Douglas-Rachford splitting holds when applying ADMM to the preconditioned primal, which is given by the iterations:

$$\begin{aligned} y^{k+1} &= \underset{y}{\operatorname{argmin}} \{g(y) + \frac{\gamma}{2}\|Ey - EAx^k + \lambda z^k\|^2\} \\ v^{k+1} &= 2\alpha Dy^{k+1} + (1 - 2\alpha)DAx^k \\ x^{k+1} &= \underset{x}{\operatorname{argmin}} \{f(x) + \frac{\gamma}{2}\|EAx - v^{k+1} - \gamma\lambda^k\|^2\} \\ \lambda^{k+1} &= \lambda^k + \gamma(v^{k+1} - EAx^{k+1}) \end{aligned}$$

Thus, the optimal preconditioner E in ADMM under Assumption 3 is computed by solving (18), subject to E diagonal, and the optimal choice of γ is $\gamma = \frac{1}{\sqrt{\lambda_{\max}(EAH^{-1}A^TE^T)\lambda_{\min}(EAL^{-1}A^TE^T)}}$, and the optimal $\alpha = 1$. Note that the γ -parameter in ADMM is in the numerator, while the same γ -parameter in dual Douglas-Rachford splitting is in the denominator.

Remark 3: This preconditioning result is a generalization of the result in [19] where the restricted case of $f(x) = \frac{1}{2}x^T Hx + h^T x$ and $g(y) = I_{y \leq d}(y)$ is considered.

VI. HEURISTIC METRIC SELECTION

In this section, we discuss metric and parameter selection when some of the assumptions needed to have linear convergence are not met. We focus here on quadratic problems of the form

$$\text{minimize} \quad \underbrace{\frac{1}{2}x^T Qx + q^T x + \hat{f}(x)}_{f(x)} + g(Ax) \quad (21)$$

where $Q \in \mathbf{S}_+^n$, $q \in \mathbf{R}^n$, $\hat{f} \in \Gamma_0(\mathbf{R}^n)$, $g \in \Gamma_0(\mathbf{R}^n)$ and $A \in \mathbf{R}^{m \times n}$. One set of assumptions that guarantee linear convergence for Douglas-Rachford splitting applied to the primal or the dual is that Q is positive definite, $\hat{f} \equiv 0$, and that A has full row rank. Here, we consider situations in which some of these assumptions are not met. Specifically, we consider situations where (some of) the following items violate the linear convergence assumptions:

- (i) $Q \in \mathbf{S}_+^n$ is not positive definite, but positive semi-definite.
- (ii) $\hat{f} \neq 0$, but instead the indicator function of a convex constraint set (or some other non-smooth function without curvature).
- (iii) $A \in \mathbf{R}^{m \times n}$ does not have full row rank.

In the first case, we lose strong convexity in the primal formulation and smoothness in the dual formulation. In the second case, we lose smoothness in the primal formulation and strong convexity in the dual formulation. The third case

is not applicable to the primal case (since $A = I$ there), but in the dual formulation this results in loss of strong convexity.

We first discuss the primal formulation and assume that the assumptions that give linear convergence are violated using both (i) and (ii). Then, we have quadratic curvature only in the range space of Q . In the null space of Q , the function f is governed by the function \hat{f} (which is either 0 or ∞ if it is the indicator function of a convex constraint set). Therefore, we propose to select a diagonal metric $M = (D^T D)^{-1}$ that optimizes the conditioning on the range space of Q , i.e., that solves

$$\text{minimize} \quad \frac{\lambda_{\max}(D^T Q D)}{\lambda_{\min>0}(D^T Q D)}$$

where $\lambda_{\min>0}$ denotes the smallest non-zero eigenvalue. Also, we propose to select the γ -parameter to reflect the curvature on the range space of Q , i.e., $\gamma = \frac{1}{\sqrt{\lambda_{\max}(D^T Q D)\lambda_{\min>0}(D^T Q D)}}$.

For the dual case, i.e., the ADMM case, we propose to select the metric as if $\hat{f} \equiv 0$ (which it is if the assumptions to get linear convergence are not violated by point (ii)). To do this, we define the quadratic part of f in (21) to be $f_{\text{pc}}(x) := \frac{1}{2}x^T Qx + q^T x$ and introduce the function $d_{\text{pc}} = f_{\text{pc}}^* \circ -A^T$. The heuristic metric selection will be based on this function. The function f_{pc} is given by

$$\begin{aligned} f_{\text{pc}}^*(y) &= \sup_x \{\langle y, x \rangle - f_{\text{pc}}(x)\} \\ &= \begin{cases} \frac{1}{2}(y - q)^T Q^\dagger (y - q) & \text{if } (y - q) \in \mathcal{R}(Q) \\ \infty & \text{else} \end{cases} \end{aligned}$$

where Q^\dagger is the pseudo-inverse of Q and \mathcal{R} denotes the range space. This gives

$$d_{\text{pc}}(\mu) = \begin{cases} \frac{1}{2}(A^T \mu + q)^T Q^\dagger (A^T \mu - q) & \text{if } (A^T \mu + q) \in \mathcal{R}(Q) \\ \infty & \text{else} \end{cases}$$

The quadratic part of the approximated dual d_{pc} is given by $AQ^\dagger A^T$, and is defined on a sub-space only (if Q is not positive definite). As in the primal case, we propose to select a diagonal metric $K = E^T E$ such that the quadratic part of the, in some cases approximate, dual function is well conditioned on its domain. That is, we propose to select a metric such that the pseudo condition number of $AQ^\dagger A^T$ is minimized, i.e., a diagonal metric E that is computed by solving

$$\text{minimize} \quad \frac{\lambda_{\max}(EAQ^\dagger A^T E^T)}{\lambda_{\min>0}(EAQ^\dagger A^T E^T)}.$$

This reduces to the optimal metric choice in the case where linear convergence is achieved, i.e., where none of items (i), (ii), or (iii) are met, and can be used as a heuristic when any of the points (i), (ii), and/or (iii) violates the assumptions needed to get linear convergence. The γ -parameter is also chosen to in accordance with the above reasoning and Corollary 2 as $\gamma = \frac{1}{\sqrt{\lambda_{\max}(EAQ^\dagger A^T E^T)\lambda_{\min>0}(EAQ^\dagger A^T E^T)}}$.

In the particular case where \hat{f} in (21) is the indicator function for an affine subspace, i.e., when $\hat{f} = I_{Bx=b}$. Then d can be written as

$$d(\mu) = \frac{1}{2}\mu^T AP_{11}A^T \mu + \xi^T \mu + \chi$$

where $\xi \in \mathbf{R}^n$, $\chi \in \mathbf{R}$, and

$$\begin{bmatrix} Q & B^T \\ B & 0 \end{bmatrix}^{-1} = \begin{bmatrix} P_{11} & P_{12} \\ P_{21} & P_{22} \end{bmatrix}.$$

Then we can choose metric by minimizing the pseudo condition number of $AP_{11}A^T$, which is the Hessian of d , and select γ as $\gamma = \frac{1}{\sqrt{\lambda_{\max}(EAP_{11}A^TE^T)\lambda_{\min>0}(EAP_{11}A^TE^T)}}$.

Minimization of the pseudo condition number $\lambda_{\max}/\lambda_{\min>0}$ can be posed as a convex optimization problem and be solved exactly, see [21, Section 6]. Also computationally cheap heuristics to select E that reduce the pseudo condition number can be found there.

VII. NUMERICAL EXAMPLE

In this section, we evaluate the metric and parameter selection method by applying ADMM to the (small-scale) aircraft control problem from [28], [5]. As in [5], the continuous time model from [28] is sampled using zero-order hold every 0.05 s. The system has four states $x = (x_1, x_2, x_3, x_4)$, two outputs $y = (y_1, y_2)$, two inputs $u = (u_1, u_2)$, and obeys the following dynamics

$$x^+ = \begin{bmatrix} 0.999 & -3.008 & -0.113 & -1.608 \\ -0.000 & 0.986 & 0.048 & 0.000 \\ 0.000 & 2.083 & 1.009 & -0.000 \\ 0.000 & 0.053 & 0.050 & 1.000 \end{bmatrix} x + \begin{bmatrix} -0.080 & -0.635 \\ -0.029 & -0.014 \\ -0.868 & -0.092 \\ -0.022 & -0.002 \end{bmatrix} u,$$

$$y = \begin{bmatrix} 0 & 1 & 0 & 0 \\ 0 & 0 & 0 & 1 \end{bmatrix} x$$

where x^+ denotes the state in the next time step. The system is unstable, the magnitude of the largest eigenvalue of the dynamics matrix is 1.313. The outputs are the attack and pitch angles, while the inputs are the elevator and flaperon angles. The inputs are physically constrained to satisfy $|u_i| \leq 25^\circ$, $i = 1, 2$. The outputs are soft constrained to satisfy $-s_1 - 0.5 \leq y_1 \leq 0.5 + s_2$ and $-s_3 - 100 \leq y_2 \leq 100 + s_4$ respectively, where $s = (s_1, s_2, s_3, s_4) \geq 0$ are slack variables. The cost in each time step is

$$\ell(x, u, s) = \frac{1}{2}((x - x_r)^T Q (x - x_r) + u^T R u + s^T S s)$$

where x_r is a reference, $Q = \text{diag}(10^{-4}, 10^2, 10^{-3}, 10^2)$, $R = 10^{-2}I$, and $S = 10^6I$. This gives a condition number of 10^{10} of the full cost matrix. Further, the terminal cost is Q , and the control and prediction horizon is $N = 10$. The numerical data in Figure 5 is obtained by following a reference trajectory on the output. The objective is to change the pitch angle from 0° to 10° and then back to 0° while the angle of attack satisfies the output constraints $-0.5^\circ \leq y_1 \leq 0.5^\circ$. The constraints on the angle of attack limits the rate on how fast the pitch angle can be changed. The full optimization problem can be written on the form

$$\begin{aligned} & \text{minimize} && \underbrace{\frac{1}{2}z^T H z + r_t^T z + I_{Bz=bx_t}(z)}_{f(z)} + \underbrace{I_{d \leq y \leq \bar{d}}(z')}_{g(z')} \\ & \text{subject to} && Cz = z' \end{aligned}$$

where x_t and r_t may change from one sampling instant to the next.

This is the optimization problem formulation discussed in Section VI where item (ii) violates the assumptions that guarantee linear convergence. In Figure 5, the performance of

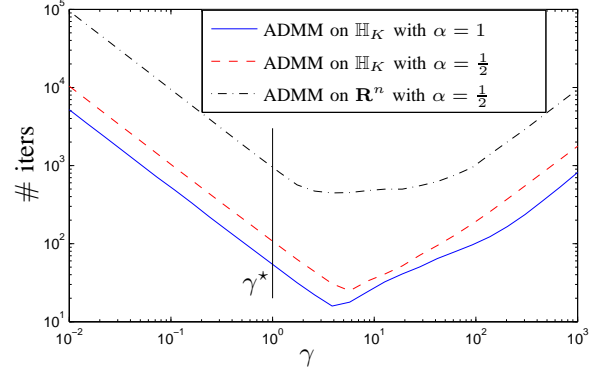


Fig. 5. Average number of iterations for different γ -values, different metrics, and different relaxations α .

the ADMM algorithm for different values of γ and for different metrics is presented. Since the numerical example treated here is a model predictive control application, we can spend much computational effort offline to compute a metric that will be used in all samples in the online controller. We compute a metric $K = E^T E$ that minimizes the condition number of $ECH^{-1}C^T E^T$ (minimization of the pseudo condition number of $ECP_{11}C^T E^T$ gives about the same performance and is therefore omitted) that defines the space \mathbb{H}_K . In Figure 5, the performance of ADMM when applied on \mathbb{H}_K with relaxations $\alpha = \frac{1}{2}$ and $\alpha = 1$, and ADMM applied on \mathbf{R}^n with $\alpha = \frac{1}{2}$ is shown. In this particular example, improvements of about one order of magnitude are achieved when applied on \mathbb{H}_K compared to when applied on \mathbf{R}^n . Figure 5 also shows that ADMM with over-relaxation performs better than standard ADMM with no relaxation. The empirically best average iteration count for ADMM on \mathbb{H}_K with $\alpha = 1$ is 15.9 iterations, for ADMM on \mathbb{H}_K with $\alpha = \frac{1}{2}$ is 24.9 iterations, and for ADMM on \mathbf{R}^n with $\alpha = \frac{1}{2}$, (which is essentially the algorithm proposed in [33]), is 446.1 iterations. The proposed γ -parameter selection is denoted by γ^* in Figure 5 (E or C is scaled to get $\gamma^* = 1$ for all examples). Figure 5 shows that γ^* does not coincide with the empirically found best γ , but still gives a reasonable choice of γ in all cases.

VIII. CONCLUSIONS

We have presented methods to select metric and parameters for Douglas-Rachford splitting, Peaceman-Rachford splitting and ADMM. We have also provided a numerical example to evaluate the proposed metric and parameter selection methods for ADMM. Performance improvements of about one order of magnitude, compared to when ADMM is applied on the Euclidean space, are reported.

REFERENCES

- [1] K. J. Arrow, L. Hurwicz, and H. Uzawa. *Studies in Linear and Nonlinear Programming*. Stanford University Press, 1958.
- [2] J.-B. Baillon and G. Haddad. Quelques propriétés des opérateurs angle-bornés etn-cycliquement monotones. *Israel Journal of Mathematics*, 26(2):137–150, 1977.
- [3] H. H. Bauschke and P. L. Combettes. *Convex Analysis and Monotone Operator Theory in Hilbert Spaces*. Springer, 2011.

- [4] A. Beck and M. Teboulle. A fast iterative shrinkage-thresholding algorithm for linear inverse problems. *SIAM J. Imaging Sciences*, 2(1):183–202, 2009.
- [5] A. Bemporad, A. Casavola, and E. Mosca. Nonlinear control of constrained linear systems via predictive reference management. *IEEE Transactions on Automatic Control*, 42(3):340–349, 1997.
- [6] D. Boley. Local linear convergence of the alternating direction method of multipliers on quadratic or linear programs. *SIAM Journal on Optimization*, 23(4):2183–2207, 2013.
- [7] S. Boyd, N. Parikh, E. Chu, B. Peleato, and J. Eckstein. Distributed optimization and statistical learning via the alternating direction method of multipliers. *Foundations and Trends in Machine Learning*, 3(1):1–122, 2011.
- [8] E. J. Candes, J. Romberg, and T. Tao. Robust uncertainty principles: exact signal reconstruction from highly incomplete frequency information. *IEEE Transactions on Information Theory*, 52(2):489–509, Feb 2006.
- [9] A. Chambolle and T. Pock. A first-order primal-dual algorithm for convex problems with applications to imaging. *Journal of Mathematical Imaging and Vision*, 40(1):120–145, 2011.
- [10] P. L. Combettes and V. R. Wajs. Signal recovery by proximal forward-backward splitting. *SIAM journal on Multiscale Modeling and Simulation*, 4(4):1168–1200, 2005.
- [11] D. Davis and W. Yin. Convergence rate analysis of several splitting schemes. Available <http://arxiv.org/abs/1406.4834>, August 2014.
- [12] D. Davis and W. Yin. Faster convergence rates of relaxed Peaceman-Rachford and ADMM under regularity assumptions. Available: <http://arxiv.org/abs/1407.5210>, July 2014.
- [13] L. Demanet and X. Zhang. Eventual linear convergence of the Douglas-Rachford iteration for basis pursuit. Available: <http://arxiv.org/abs/1301.0542>, May 2013.
- [14] W. Deng and W. Yin. On the global and linear convergence of the generalized alternating direction method of multipliers. Technical Report CAAM 12-14, Rice University, 2012.
- [15] J. Douglas and H. H. Rachford. On the numerical solution of heat conduction problems in two and three space variables. *Trans. Amer. Math. Soc.*, 82:421–439, 1956.
- [16] J. Eckstein. *Splitting methods for monotone operators with applications to parallel optimization*. PhD thesis, MIT, 1989.
- [17] D. Gabay. Applications of the method of multipliers to variational inequalities. In M. Fortin and R. Glowinski, editors, *Augmented Lagrangian Methods: Applications to the Solution of Boundary-Value Problems*. North-Holland: Amsterdam, 1983.
- [18] D. Gabay and B. Mercier. A dual algorithm for the solution of nonlinear variational problems via finite element approximation. *Computers and Mathematics with Applications*, 2(1):17–40, 1976.
- [19] E. Ghadimi, A. Teixeira, I. Shames, and M. Johansson. Optimal parameter selection for the alternating direction method of multipliers (ADMM): Quadratic problems. 2013. Submitted. Available: <http://arxiv.org/abs/1306.2454>.
- [20] P. Giselsson and S. Boyd. Diagonal scaling in Douglas-Rachford splitting and ADMM. In *53rd IEEE Conference on Decision and Control*, Los Angeles, CA, December 2014. Accepted for publication.
- [21] P. Giselsson and S. Boyd. Metric selection in fast dual gradient methods. 2014. Submitted.
- [22] R. Glowinski and A. Marroco. Sur l’approximation, par éléments finis d’ordre un, et la résolution, par pénalisation-dualité d’une classe de problèmes de dirichlet non linéaires. *ESAIM: Mathematical Modelling and Numerical Analysis - Modélisation Mathématique et Analyse Numérique*, 9:41–76, 1975.
- [23] T. Hastie, R. Tibshirani, and J. Friedman. *The elements of statistical learning: data mining, inference and prediction*. Springer, 2nd edition, 2009.
- [24] B. He and X. Yuan. On the $o(1/n)$ convergence rate of the Douglas-Rachford alternating direction method. *SIAM Journal on Numerical Analysis*, 50(2):700–709, 2012.
- [25] R. Hesse, D. R. Luke, and P. Neumann. Alternating projections and Douglas-Rachford for sparse affine feasibility. *IEEE Transactions on Signal Processing*, 62(18):4868–4881, September 2014.
- [26] M. Hong and Z.-Q. Luo. On the linear convergence of the alternating direction method of multipliers. Available: <http://arxiv.org/abs/1208.3922>, March 2013.
- [27] F. Iutzeler, P. Bianchi, P. Ciblat, and W. Hachem. Explicit convergence rate of a distributed alternating direction method of multipliers. Available: <http://arxiv.org/abs/1312.1085>, December 2013.
- [28] P. Kamasouris, M. Athans, and G. Stein. Design of feedback control systems for unstable plants with saturating actuators. In *Proceedings of the IFAC Symposium on Nonlinear Control System Design*, pages 302–307. Pergamon Press, 1990.
- [29] P. L. Lions and B. Mercier. Splitting algorithms for the sum of two nonlinear operators. *SIAM Journal on Numerical Analysis*, 16(6):964–979, 1979.
- [30] M. Lustig, D. Donoho, and J. M. Pauly. Sparse MRI: The application of compressed sensing for rapid MR imaging. *Magnetic Resonance in Medicine*, 58(6):1182–1195, 2007.
- [31] Y. Nesterov. *Introductory Lectures on Convex Optimization: A Basic Course*. Springer Netherlands, 1st edition, 2003.
- [32] R. Nishihara, L. Lessard, B. Recht, A. Packard, and M. Jordan. A general analysis of the convergence of ADMM. February 2015. Available: <http://arxiv.org/abs/1502.02009>.
- [33] B. O’Donoghue, G. Stathopoulos, and S. Boyd. A splitting method for optimal control. *IEEE Transactions on Control Systems Technology*, 21(6):2432–2442, 2013.
- [34] N. Parikh and S. Boyd. Proximal algorithms. *Foundations and Trends in Optimization*, 1(3):123–231, 2014.
- [35] P. Patrinos, L. Stella, and A. Bemporad. Douglas-Rachford splitting: Complexity estimates and accelerated variants. In *Proceedings of the 53rd IEEE Conference on Decision and Control*, Los Angeles, CA, December 2014.
- [36] D. W. Peaceman and H. H. Rachford. The numerical solution of parabolic and elliptic differential equations. *Journal of the Society for Industrial and Applied Mathematics*, 3(1):28–41, 1955.
- [37] H. M. Phan. Linear convergence of the Douglas-Rachford method for two closed sets. Available: <http://arxiv.org/abs/1401.6509>, October 2014.
- [38] A. Raghunathan and S. Di Cairano. ADMM for convex quadratic programs: Linear convergence and infeasibility detection. November 2014. Available: <http://arxiv.org/abs/1411.7288>.
- [39] J. B. Rawlings and D. Q. Mayne. *Model Predictive Control: Theory and Design*. Nob Hill Publishing, Madison, WI, 2009.
- [40] R. T. Rockafellar and R. J-B. Wets. *Variational Analysis*. Springer, Berlin, 1998.
- [41] W. Shi, Q. Ling, K. Yuan, G. Wu, and W. Yin. On the linear convergence of the ADMM in decentralized consensus optimization. *IEEE Transactions on Signal Processing*, 62(7):1750–1761, April 2014.
- [42] R. Tibshirani. Regression shrinkage and selection via the lasso. *J. Royal. Statist. Soc. B.*, 58(1):267–288, 1996.

APPENDIX A PROOF OF PROPOSITION 5

Proof. The direction (i) \Rightarrow (ii) follows, without any changes, by stating [31, Lemma 1.2.3] on general real Hilbert spaces instead of in an Euclidean setting.

To show (ii) \Rightarrow (i), we add two copies of the smoothness definition in (2) with x and y interchanged to get:

$$|f(x) - f(y) - \langle \nabla f(y), x - y \rangle| \tag{22}$$

$$+ |f(y) - f(x) - \langle \nabla f(x), y - x \rangle| \leq \beta \|x - y\|^2.$$

For each pair of points (x, y) , the possible combinations of signs of the expressions inside the absolute values are: $(+, +)$, $(+, -)$, $(-, +)$, or $(-, -)$. For $(+, +)$, and $(-, -)$, we get

$$|\langle \nabla f(x) - \nabla f(y), x - y \rangle| \leq \beta \|x - y\|^2.$$

In the situations where the signs are $(+, -)$, the expression (22) reduces to:

$$2f(x) - 2f(y) - \langle \nabla f(y) + \nabla f(x), x - y \rangle \leq \beta \|x - y\|^2. \tag{23}$$

Since, by assumption $f(x) - f(y) - \langle \nabla f(y), x - y \rangle \geq 0$ (the expression in the first absolute value in (22) is nonnegative since we treat the situation $(+, -)$) we have:

$$2(f(x) - f(y)) \geq 2\langle \nabla f(y), x - y \rangle.$$

Thus

$$\begin{aligned} & \langle \nabla f(y) - \nabla f(x), x - y \rangle \\ &= -\langle \nabla f(x) + \nabla f(y), x - y \rangle + 2\langle \nabla f(y), x - y \rangle \\ &\leq 2f(x) - 2f(y) - \langle \nabla f(y) + \nabla f(x), x - y \rangle \leq \beta \|x - y\|^2 \end{aligned}$$

where the last inequality is due to (23). The situation with $(-, +)$ gives the same inequality by interchanging the place of x and y . Thus, for any of the four scenarios, we have

$$|\langle \nabla f(x) - \nabla f(y), x - y \rangle| \leq \beta \|x - y\|^2.$$

Now, apply Cauchy-Schwarz inequality to get

$$\|\nabla f(x) - \nabla f(y)\| \leq \beta \|x - y\|.$$

This completes the proof. \square

APPENDIX B

PROOF OF PROPOSITION 13

Proof. Define $\hat{f} = 2f_\gamma^* - \frac{1}{2}\|\cdot\|^2$ (where f_γ is defined in (4)). Through Proposition 8, we get that $\nabla \hat{f} = 2\nabla f_\gamma^* - I = 2\text{prox}_{\gamma f} - I = R_{\gamma f}$. We get

$$\begin{aligned} \langle \nabla \hat{f}(y), x - y \rangle &= \langle 2\nabla f_\gamma^*(y) - y, x - y \rangle \\ &\leq 2(f_\gamma^*(x) - f_\gamma^*(y) - \frac{1}{2(\gamma\beta+1)}\|x - y\|^2) \\ &\quad - (\frac{1}{2}\|x\|^2 - \frac{1}{2}\|y\|^2 - \frac{1}{2}\|x - y\|^2) \\ &= \hat{f}(x) - \hat{f}(y) + \frac{\gamma\beta-1}{2(\gamma\beta+1)}\|x - y\|^2 \end{aligned}$$

where Proposition 10 and Proposition 4 are used in the inequality. We also have

$$\begin{aligned} \langle \nabla \hat{f}(y), x - y \rangle &= \langle 2\nabla f_\gamma^*(y) - y, x - y \rangle \\ &\geq 2(f_\gamma^*(x) - f_\gamma^*(y) - \frac{1}{2(\gamma\sigma+1)}\|x - y\|^2) \\ &\quad - (\frac{1}{2}\|x\|^2 - \frac{1}{2}\|y\|^2 - \frac{1}{2}\|x - y\|^2) \\ &= \hat{f}(x) - \hat{f}(y) + \frac{\gamma\sigma-1}{2(\gamma\sigma+1)}\|x - y\|^2 \end{aligned}$$

where Proposition 9 and Proposition 4 are used in the inequality. This implies that

$$\begin{aligned} \frac{\gamma\sigma-1}{2(\gamma\sigma+1)}\|x - y\|^2 &\leq \langle \nabla \hat{f}(y), x - y \rangle + \hat{f}(y) - \hat{f}(x) \\ &\leq \frac{\gamma\beta-1}{2(\gamma\beta+1)}\|x - y\|^2 \end{aligned}$$

or equivalently (by negating the first inequality)

$$\begin{aligned} |\langle \nabla \hat{f}(y), x - y \rangle + \hat{f}(y) - \hat{f}(x)| \\ \leq \frac{1}{2} \max\left(\frac{\gamma\beta-1}{\gamma\beta+1}, \frac{1-\gamma\sigma}{\gamma\sigma+1}\right) \|x - y\|^2. \end{aligned} \quad (24)$$

Since $\nabla \hat{f} = R_{\gamma f}$, the result follows from Proposition 5. \square

APPENDIX C

PROOF OF PROPOSITION 14

Proof. By [3, Corollary 23.10] R_B is nonexpansive and by Proposition 12 R_A is $\delta = \sqrt{1 - \frac{4\gamma\sigma}{(1+\gamma\beta)^2}}$ -contractive. Thus the composition $R_A R_B$ is also δ -contractive since

$$\|R_A R_B z_1 - R_A R_B z_2\| \leq \delta \|R_B z_1 - R_B z_2\| \leq \delta \|z_1 - z_2\|. \quad (25)$$

Now, let $T = (1 - \alpha)I + \alpha R_A R_B$ be the generalized Douglas-Rachford operator in (6). Since \bar{z} is a fixed-point of $R_A R_B$ it is also a fixed-point of T , i.e., $\bar{z} = T\bar{z}$. Thus

$$\begin{aligned} \|z^{k+1} - \bar{z}\| &= \|Tz^k - T\bar{z}\|^2 \\ &= \|(1 - \alpha)(z^k - \bar{z}) + \alpha(R_A R_B z^k - R_A R_B \bar{z})\| \\ &\leq |1 - \alpha| \|z^k - \bar{z}\| + \alpha \|R_A R_B z^k - R_A R_B \bar{z}\| \\ &\leq (|1 - \alpha| + \alpha\delta) \|z^k - \bar{z}\| \\ &= \left(|1 - \alpha| + \alpha\sqrt{1 - \frac{4\gamma\sigma}{(1+\gamma\beta)^2}}\right) \|z^k - \bar{z}\| \end{aligned}$$

where (25) is used in the second inequality. This concludes the proof. \square